Nup2 requires a highly divergent partner, NupA, to fulfill functions at nuclear pore complexes and the mitotic chromatin region

Sarine Markossian[a], Subbulakshmi Suresh[b], Aysha H. Osmani[b], and Stephen A. Osmani[b]
[a]Laboratory of Gene Regulation and Development, National Institute for Child Health and Human Development, National Institutes of Health, Bethesda, MD 20892; [b]Department of Molecular Genetics, Ohio State University, Columbus, OH 43210

ABSTRACT **Chromatin and nuclear pore complexes (NPCs) undergo dramatic changes during mitosis, which in vertebrates and *Aspergillus nidulans* involves movement of Nup2 from NPCs to the chromatin region to fulfill unknown functions. This transition is shown to require the Cdk1 mitotic kinase and be promoted prematurely by ectopic expression of the NIMA kinase. Nup2 localizes with a copurifying partner termed NupA, a highly divergent yet essential NPC protein. NupA and Nup2 locate throughout the chromatin region during prophase but during anaphase move to surround segregating DNA. NupA function is shown to involve targeting Nup2 to its interphase and mitotic locations. Deletion of either Nup2 or NupA causes identical mitotic defects that initiate a spindle assembly checkpoint (SAC)–dependent mitotic delay and also cause defects in karyokinesis. These mitotic problems are not caused by overall defects in mitotic NPC disassembly–reassembly or general nuclear import. However, without Nup2 or NupA, although the SAC protein Mad1 locates to its mitotic locations, it fails to locate to NPCs normally in G1 after mitosis. Collectively the study provides new insight into the roles of Nup2 and NupA during mitosis and in a surveillance mechanism that regulates nucleokinesis when mitotic defects occur after SAC fulfillment.**

Monitoring Editor
Karsten Weis
ETH Zurich

Received: Sep 9, 2014
Revised: Dec 5, 2014
Accepted: Dec 17, 2014

INTRODUCTION

Nuclear pore complexes (NPCs) are large macromolecular assemblies spanning the nuclear envelope (NE) composed of multiple copies of proteins termed nucleoporins, commonly abbreviated to Nups. NPCs form channels across the NE that bridge the nucleoplasm and cytoplasm, allowing the diffusion of small molecules and active transport of larger proteins and nucleic acids (Alber *et al.*, 2007; Stewart, 2007; D'Angelo and Hetzer, 2008). The core structure of the NPC is anchored in the NE via transmembrane Nups in combination with core subcomplexes. Additional peripheral Nups form a nuclear basket and cytoplasmic fibrils, whereas peripheral phenylalanine-glycine (FG)–repeat Nups reside within the central transport channel (Strambio-De-Castillia *et al.*, 2010; Wente and Rout, 2010; Raices and D'Angelo, 2012; Schwartz, 2013). FG-repeat Nups of the central transport channel are intrinsically disordered and can form hydrogel-like barriers (Frey *et al.*, 2006; Frey and Gorlich, 2007). Cargo–carrier complexes are docked and translocate through the NPC via interactions between importin or exportin carriers and the FG-repeat proteins (Bayliss *et al.*, 2000).

During open-type mitosis when NPCs undergo disassembly, several Nups have been shown to locate to kinetochores, spindle pole bodies, and mitotic chromatin (Belgareh *et al.*, 2001; Harel *et al.*, 2003; Loiodice *et al.*, 2004; Galy *et al.*, 2006; Orjalo *et al.*, 2006; Osmani *et al.*, 2006a; Rasala *et al.*, 2006; Liu *et al.*, 2009; Xu and Powers, 2010), indicating that Nups have evolved to mediate mitotic functions away from NPCs (De Souza and Osmani, 2007, 2009; Guttinger *et al.*, 2009; Bolhy *et al.*, 2011). Nups including Rae1, Nup98, and components of the core Nup107/160 subcomplex regulate spindle formation and anaphase onset in *Xenopus* extracts, *Caenorhabditis elegans*, mice, and human cells (Kraemer *et al.*, 2001; Joseph *et al.*, 2002; Pichler *et al.*, 2002; Arnaoutov *et al.*, 2005;

This article was published online ahead of print in MBoC in Press (http://www.molbiolcell.org/cgi/doi/10.1091/mbc.E14-09-1359) on December 24, 2014.
Address correspondence to: Stephen A. Osmani (osmani.2@osu.edu).
Abbreviations used: ChRFP, mCherry variant of red fluorescent protein; DAPI, 4′,6-diamidino-2-phenylindole; ETOH, ethanol; HU, hydroxyurea; Kap, karyopherin; NE, nuclear envelope; NIMA, never In mitosis A; NLS, nuclear localization signal; NPC, nuclear pore complex; Nup, nucleoporin; SAC, spindle assembly checkpoint.

Blower *et al.*, 2005; Jeganathan *et al.*, 2005, 2006; Orjalo *et al.*, 2006; Wong *et al.*, 2006; Zuccolo *et al.*, 2007; Platani *et al.*, 2009; Mishra *et al.*, 2010; Cross and Powers, 2011). In addition, the NPC nuclear basket protein Nup153 is required for early mitotic progression, as well as for the resolution of midbodies during cytokinesis in HeLa cells (Mackay *et al.*, 2009). Nup153 depletion leads to defects in NPC basket assembly and activates an Aurora B–mediated abscission checkpoint (Mackay *et al.*, 2010). Moreover, the spindle assembly checkpoint (SAC) proteins Mad1 and Mad2 locate to the NPC nuclear basket in mammalian cells (Campbell *et al.*, 2001), *Saccharomyces cerevisiae* (Iouk *et al.*, 2002), *Aspergillus nidulans* (De Souza *et al.*, 2009), plant cells (Ding *et al.*, 2012), and *Drosophila melanogaster* (Buffin *et al.*, 2005; Katsani *et al.*, 2008), suggesting a conserved functional relationship between the SAC and NPCs. A recent study also found that during interphase, NPCs provide a platform for generation of mitotic Mad2-inhibitory complexes previously believed to be generated exclusively from incorrectly attached mitotic kinetochores (Rodriguez-Bravo *et al.*, 2014). In *A. nidulans*, the nuclear basket protein Mlp1, in addition to targeting Mad1 and Mad2 to interphase NPCs, also acts as a scaffold to locate Mad1 and Mad2 near kinetochores and the telophase spindle (De Souza *et al.*, 2009), similar to its human and *Drosophila* counterparts, Tpr and Mtor. Mtor promotes the recruitment of Mad2 but not Mad1 to unattached kinetochores (Lince-Faria *et al.*, 2009). Depletion of Tpr decreases the levels of Mad1 at kinetochores during prometaphase and leads to a defective SAC response (Lee *et al.*, 2008; Schweizer *et al.*, 2013).

Nup2, a mobile nucleoporin, is also part of the NPC nuclear basket. Nup2 proteins have a conserved overall domain structure divided into three domains: an N-terminal importin-α–binding domain, a domain rich in FG repeats, and a C-terminal Ran GTP–binding domain. Yeast Nup2p and the orthologous vertebrate Nup50 also contain an NPC-targeting domain, which follows the N-terminal importin-α–binding domain (Booth *et al.*, 1999; Hood *et al.*, 2000; Matsuura *et al.*, 2003; Matsuura and Stewart, 2005). Budding yeast Nup2p forms a multiprotein complex with Nup60p, Kap60 (importin-α), Kap95 (importin-β), Prp20p/RCC1, and Gsp1p/RanGTP (Allen *et al.*, 2001, 2002; Denning *et al.*, 2001, 2002; Dilworth *et al.*, 2001) and accelerates the rate of disassembly of Kap60p–cargo complexes (Gilchrist *et al.*, 2002; Gilchrist and Rexach, 2003). Nup2p facilitates this process by strongly binding to importin-α (Solsbacher *et al.*, 2000) and also participates in the nuclear export of importin-α (Booth *et al.*, 1999; Hood *et al.*, 2000). Nup50 (mammalian Nup2) also interacts with the importin-α/β–RanGTP complex to stimulate nuclear import (Lindsay *et al.*, 2002). Nup2 has additionally been implicated in gene regulation (Liang and Hetzer, 2011) and binds to a set of promoters in yeast to activate gene expression (Casolari *et al.*, 2004; Schmid *et al.*, 2006). Nup2p also acts as a physical tether for chromatin boundary activities (Ishii *et al.*, 2002) and plays an active role in the transition of chromatin between different transcriptional activity states (Dilworth *et al.*, 2005). Similarly, *Drosophila* Nup50 interacts with transcriptionally active genes (Kalverda *et al.*, 2010), although in this case, the physical interactions occur in the nucleoplasm rather than at NPCs. In addition, recent work shows that Nup50 is required for mouse myoblast differentiation and plays transport-independent roles in chromatin biology that occurs away from the NPC (Buchwalter *et al.*, 2014).

A. nidulans Nup2 also has a predicted N-terminal importin-α–binding domain (amino acids [aa] 1–50), FG repeats (3 FXFGs, 3 GXFGs, and 15 FGs), and a C-terminal Ran-GTP– binding domain (aa 1285–1404; Osmani *et al.*, 2006a) but is a significantly larger protein than its yeast and human counterparts. *A. nidulans* Nup2 is essential, and its deletion leads to mitotic DNA segregation defects. Moreover, *A. nidulans* Nup2 translocates to the main chromatin region from NPCs during mitosis (Osmani *et al.*, 2006a), a transition conserved in rat kidney cells (Dultz *et al.*, 2008). A study also identified Nup50 in the protein composition of mitotic chromosomes (Ohta *et al.*, 2010). Nup2 might therefore have as-yet-unknown but conserved roles near mitotic chromatin.

In this study, by affinity purifying *A. nidulans* Nup2, we identify a previously uncharacterized essential *A. nidulans* nucleoporin we named NupA. NupA, like Nup2, translocates from interphase NPCs to locate to the mitotic chromatin region, and both play roles during mitosis that are monitored by the SAC and are also required for normal nucleokinesis. Although neither is involved in regeneration of transport-competent NPCs after mitosis, they are required for nuclear import of Mad1 during G1.

RESULTS

Nup2 is phosphorylated when it locates to the chromatin region during mitosis

Endogenous Nup2 tagged with green fluorescent protein (GFP) is functional and translocates from NPCs to the chromatin region during mitotic entry and relocates back to NPCs during mitotic exit (Osmani *et al.*, 2006a). To determine whether Nup2 is located like Nup2-GFP, an antibody was generated and used for immunofluorescence microscopy. Similar to the GFP-tagged version, untagged Nup2 was found to locate to NPCs during interphase and the chromatin region during mitosis (Figure 1, A and B), indicating Nup2-GFP reflects the normal cell cycle– regulated locations of Nup2.

For biochemical analysis and to facilitate identification of copurifying partners via affinity purification, we generated an endogenously replaced, C-terminally S-tagged (Liu *et al.*, 2010) version of Nup2. Both Nup2-S-Tag (146 kDa) and Nup2-GFP (171 kDa) migrate at an unexpected high molecular weight during SDS–PAGE (e.g., Nup2-S-Tag runs between the 160- and 250-kDa markers; Figure 1C), as does the endogenous protein (Figure 1A). The basis for this discrepancy in apparent size is unknown. However, in addition to the aberrant large size of Nup2 during SDS–PAGE, we also observed that mitotic Nup2 (Figure 1A) and mitotic Nup2-S-Tag (Figure 1C) appeared as a smear when compared with the more defined bands of G2 samples. In vitro phosphatase treatment caused collapse of the smear to a single band, indicating that Nup2 is a mitotic phosphoprotein (Figure 1C). Because the mitotic samples were generated after release of the temperature-sensitive *nimT23* allele, the Cdc25 mitotic Cdk1–activating phosphatase in *A. nidulans* (Osmani *et al.*, 1991; O'Connell *et al.*, 1992), to a permissive temperature, the data indicate that mitotic Nup2 phosphorylation depends on mitotic Cdk1 activation (Figure 1, A and C).

A. nidulans NPCs undergo partial disassembly during mitosis, and the NIMA kinase is able to promote NPC disassembly when ectopically expressed, even during interphase (De Souza *et al.*, 2004; De Souza and Osmani, 2007). We therefore sought to determine whether NIMA could promote the removal of Nup2 from NPCs and perhaps even trigger its transition to the chromatin region. We used a strain able to express a stable kinase-active, C-terminally truncated (NIMAΔC) version of NIMA (Pu and Osmani, 1995) under control of the regulatable *alcA* promoter (Waring *et al.*, 1989). The expression of NIMAΔC was turned on in untreated cells or cells arrested in S phase by hydroxyurea (HU). The abundance of NIMAΔC and subsequent mobility shifts for endogenous NIMA and Nup2 were monitored via Western blot analysis (Figure 2A). An increase in the level of NIMAΔC occurred after 30 min of induction and accumulated further with time of induction. The increase in NIMAΔC levels correlated with mobility shifts in endogenous NIMA and

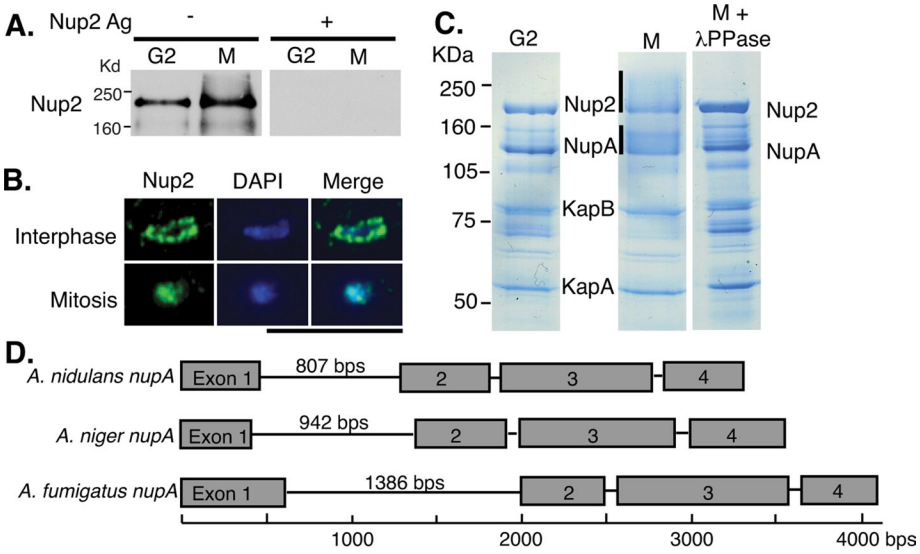

FIGURE 1: Identification of a novel Nup via affinity purification of Nup2. (A) Western blot of *A. nidulans* total cell extracts from wild-type strain R153 using Nup2 antibody pretreated with or without the Nup2 antigen (Ag) as indicated. The antibody recognizes Nup2 during both G2 and mitosis (M). (B) Cells of strain R153 were fixed and labeled with the Nup2 antibody and DAPI stained to visualize DNA. Native Nup2 is at NPCs during interphase but localized near DNA during mitosis. Scale bar, ~5 μm. (C) Coomassie-stained SDS–PAGE gel showing Nup2 copurified with a novel nucleoporin termed NupA identified by mass spectroscopy (from strain SO926). The first two samples depict affinity purifications performed for G2 and mitotic samples. The third purified mitotic sample was treated with λ phosphatase before electrophoresis. Sequence coverage obtained from mass spectroscopy: G2 sample: 72.9% for Nup2, 34.2% for NupA, 37.8% for KapB, and 36.2% for KapA; mitotic sample: 73% for Nup2, 36.7% for NupA, 34.1% for KapB, and 32.4% for KapA. (D) Cartoon depicting genomic structure of *nupA* from the indicated species. All contain a large intron between exons 1 and 2.

Nup2, indicating that extra NIMAΔC promotes the phosphorylation of both. A similar pattern was seen after induction of NIMAΔC in the presence of HU, but in this case, induction of NIMAΔC was delayed, as were the mobility shifts of endogenous NIMA and Nup2 (Figure 2A, right).

Further NIMAΔC induction experiments were completed using live-cell imaging in a strain with Nup2 tagged with GFP also expressing nuclear localization signal (NLS)–DsRed. Induction of NIMA promotes NPC disassembly and the nuclear leakage of NLS-DsRed, both normally mitotic-specific events (Suelmann *et al.*, 1997; De Souza *et al.*, 2004; Osmani *et al.*, 2006a). The ability of induced NIMAΔC to promote Nup2 to the chromatin region was monitored with or without addition of HU (Figure 2B). Representative imaging in Figure 2C shows that control cells lacking inducible NIMAΔC but treated with *alcA* inducer were not promoted into a mitotic state. However, for cells in which NIMAΔC was induced, a mitotic state was promoted, as NLS-DsRed was released from nuclei and Nup2-GFP transferred from NPCs to the chromatin region. Quantitation of the cumulative number of cells in which Nup2-GFP located to the chromatin region revealed a delay in the transition of cells into a mitotic state with HU treatment (Figure 2B). The delay is similar to the delay we observed when induction of NIMAΔC caused mobility shifts for endogenous NIMA and Nup2 (Figure 2A). Of importance, treatment with HU caused cell cycle arrest in the control strain, as these cells failed to enter mitosis in the absence of NIMAΔC induction. Collectively the analysis indicates that Nup2 normally transitions to the chromatin region under control of mitotic-specific phosphorylation, which can be artificially promoted via increased interphase induction of NIMA.

Identification of NupA via affinity purification of Nup2

Nup2-S-tag affinity purification and mass spectrometry identified importins KapA (AN2142) and KapB (AN0906; Markina-Inarrairaegui *et al.*, 2011) and two predicted hypothetical proteins, AN3174 and AN10382, as copurifying proteins from both G2 and mitotic cells. Further analysis indicated that AN3174 and AN10382 represent a single misannotated gene (Figure 1C, NupA). For example, pBLAST analysis using AN3174 and AN10382 identified a single gene in *Aspergillus fumigatus*: Afu3g13300, a predicted 140.5-kDa protein of 1299 aa. This suggests that the *A. fumigatus* gene could represent two genes, or, alternatively, AN3174 and AN10382 could represent a single gene. Consistent with the latter possibility, sequence analysis of *A. nidulans* cDNA defined a single transcript from a gene we termed *nupA*. *nupA* encodes a 768-aa protein of 84.2 kDa (Figure 1D and Supplemental Figure S1), although during SDS–PAGE, similar to Nup2, NupA ran at a higher-than-expected apparent molecular weight. This discrepancy was observed both with untagged NupA (Figure 1C) and after Western blot analysis of GFP-tagged NupA (unpublished data). Comparison between cDNA and genomic *nupA* identified three introns, the first being rather large (807 base pairs) for a fungal intron (Figure 1D and Supplemental Figure S1). The median length of *A. nidulans* introns is 59 base pairs, with 95% of introns being between 46 and 228 base pairs in length (Sibthorp *et al.*, 2013), making the large size of the *nupA* intron conspicuous. To investigate whether *A. fumigatus nupA* contains a similar large intron, we sequenced the region spanning the predicted intron from an *A. fumigatus* cDNA library. This revealed that, similar to *A. nidulans*, *nupA* of *A. fumigatus* also contains a large (1386 base pairs) intron (Figure 1D). The size of *A. fumigatus* NupA is therefore 837 aa when the intron is spliced out. Given the large size of the intron, it is somewhat surprising that the open reading frame is maintained throughout the intron sequence. For *nupA* of *Aspergillus niger* and *Aspergillus carbonarius*, RNA-sequence data also support the existence of a large *nupA* intron within these species. Similar to *A. fumigatus nupA*, these intron sequences are devoid of in-frame stop codons (Scott Baker, Pacific Northwest National Laboratory, Richland, WA, personal communication). Of interest, tBLASTn analysis at the AspGD site using the *A. fumigatus* protein encoded through the intron showed that it has 90% identity in *Neosartorya fischeri* (score, 811 bits; *E* value, 0.0) and 47% identity in *Aspergillus clavatus* (score, 318 bits; *E* value 2e-86). Additional tBLASTn analysis at the National Center for Biotechnology Information detected similar sequences only in related aspergilli. This conservation suggests that the intron is subject to evolutionary selection and that it might be translated. However, using PCR to amplify across the intron sequences and gel electrophoretic analysis, we did not detect larger transcripts reflected in *nupA* cDNAs of *A. nidulans* or *A. fumigatus*. Using different growth conditions and developmentally staged cell types might reveal unspliced transcripts capable of encoding larger NupA isoforms.

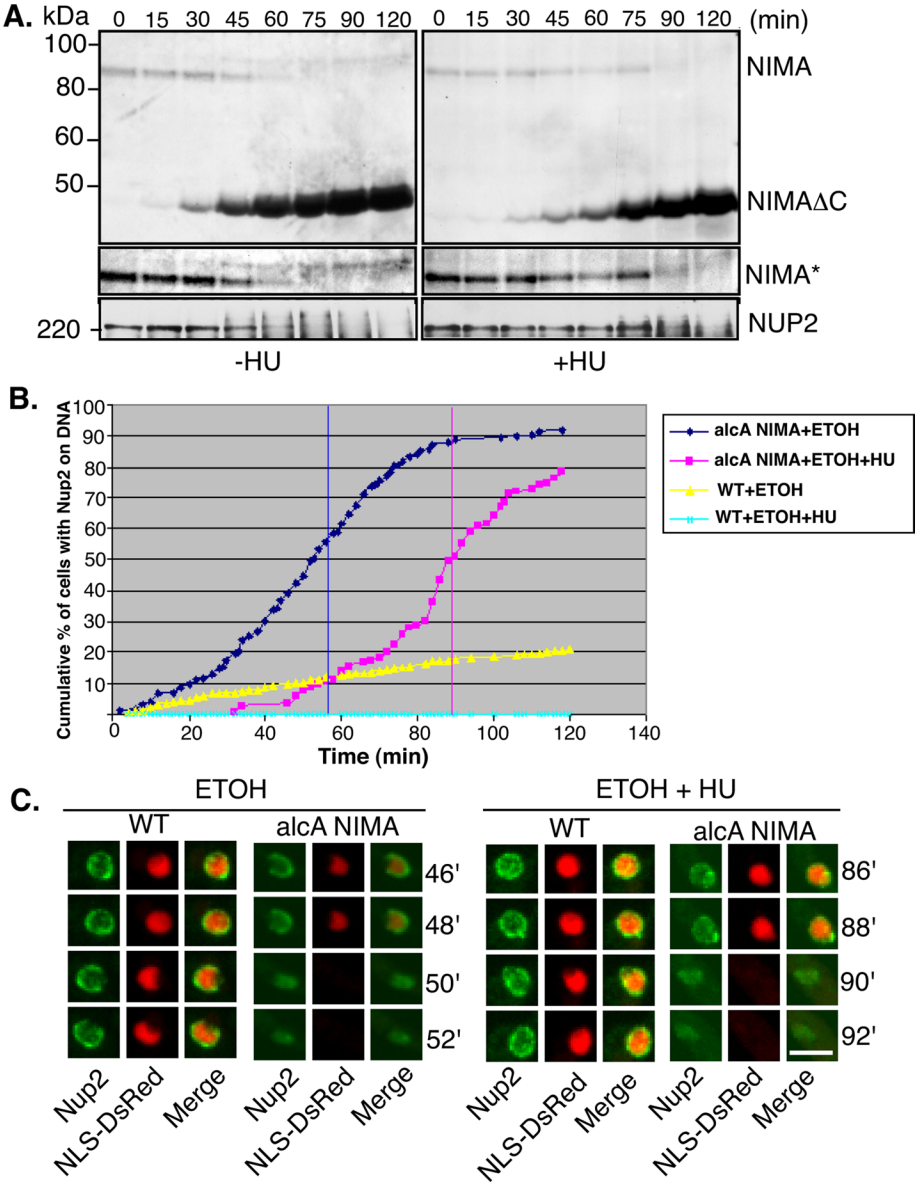

FIGURE 2: Induction of NIMA promotes phosphorylation and relocation of Nup2 from NPCs to the chromatin region even in S phase–arrested cells. (A) Western blot analysis of *A. nidulans* total cell extracts from strain SO1030 (*alcA*-NIMA) showing an upshift in Nup2 and endogenous NIMA upon induction of stable NIMA (NIMA-ΔC). NIMA*, endogenous NIMA at a higher exposure, showing its upshift upon induction of ectopic NIMA. (B) Cumulative timing of Nup2 transition from NPCs to the chromatin region upon induction of stable NIMA in the presence or absence of HU as indicated (wild-type strain HA377 and *alcA*-NIMA strain SO1030). (C) Representative images from live-cell microscopy following Nup2-GFP and NLS-DsRed with or without induction of NIMA as indicated, using strains HA377 and SO1030. Bar, ~5 μm.

NupA displays 46 and 49.5% identity at the amino acid level with its *A. fumigatus* and *A. niger* counterparts, respectively. This degree of similarity is low, as orthologues between *A. nidulans* and *A. fumigatus* average 68% amino acid identities (Galagan *et al.*, 2005). This lack of sequence conservation hindered identification of orthologues of NupA outside the aspergilli and related fungi.

NupA is essential and required for normal mitosis but not short-term growth

Deletion of *nupA* led to the generation of diploid or heterokaryotic colonies, indicating that *nupA*, although poorly conserved, is essential. Using heterokaryon rescue (Osmani *et al.*, 2006b), we identified heterokaryotic colonies that carried both Δ*nupA* and parental nuclei (Figure 3A). Diagnostic PCR confirmed the presence of the two genetically distinct types of nuclei (Figure 3Ab). Δ*nupA* mutant spores generated from the heterokaryotic colonies initially germinated and grew at a rate similar to wild-type spores but then stopped growing (Figure 3B) after several rounds of apparently defective mitosis, with nuclear DNA of the Δ*nupA* cells being missegregated and often clustered (Figure 3C). These phenotypes are very similar to the Δ*nup2* mutant (Osmani *et al.*, 2006a), suggesting that Nup2 and NupA could have interdependent functions.

Nup2 and NupA transfer from NPCs to the chromatin region in early prophase and to the chromatin periphery during anaphase

As mentioned above, during *A. nidulans* mitosis, NPCs partially disassemble, and nuclear proteins, such as NLS-DsRed, disperse from nuclei and locate throughout the cell (De Souza *et al.*, 2004; Osmani *et al.*, 2006a; De Souza and Osmani, 2009). Dispersal of NLS-DsRed therefore acts as a marker for entry into mitosis and its nuclear reimport a marker for mitotic exit into G1. In a manner identical to Nup2, NupA-GFP was found to translocate from NPCs to concentrate to the mitotic chromatin region until cells exit mitosis (Figure 4A). Accordingly, NupA-GFP and the chromatin marker histone H1–monomeric red fluorescent protein (mRFP) localized together during mitosis (Figure 4B), and, as expected from their copurification, NupA-GFP and Nup2-ChRFP localize together at interphase NPCs and the mitotic chromatin region (Figure 4C).

By observing individual confocal slices of either Nup2-GFP or NupA-GFP and histone H1-mRFP, we found that both Nup2 and NupA locate throughout the chromatin region during metaphase but transition to the periphery of chromatin during anaphase–telophase (Figure 4, D and E, and Supplemental Figure S2, A and B). Nup2 and NupA therefore undergo a biphasic transition in relationship to chromatin during mitosis. They first move from NPCs to locate throughout the mitotic chromatin region during prophase and metaphase, and then undergo a second transition during anaphase–telophase to move to a position around the periphery of the condensed separating genomes.

NupA is required for Nup2 location at NPCs and the mitotic chromatin region

Because Nup2 and NupA display identical dynamic subcellular localizations and cause similar mitotic defects when deleted

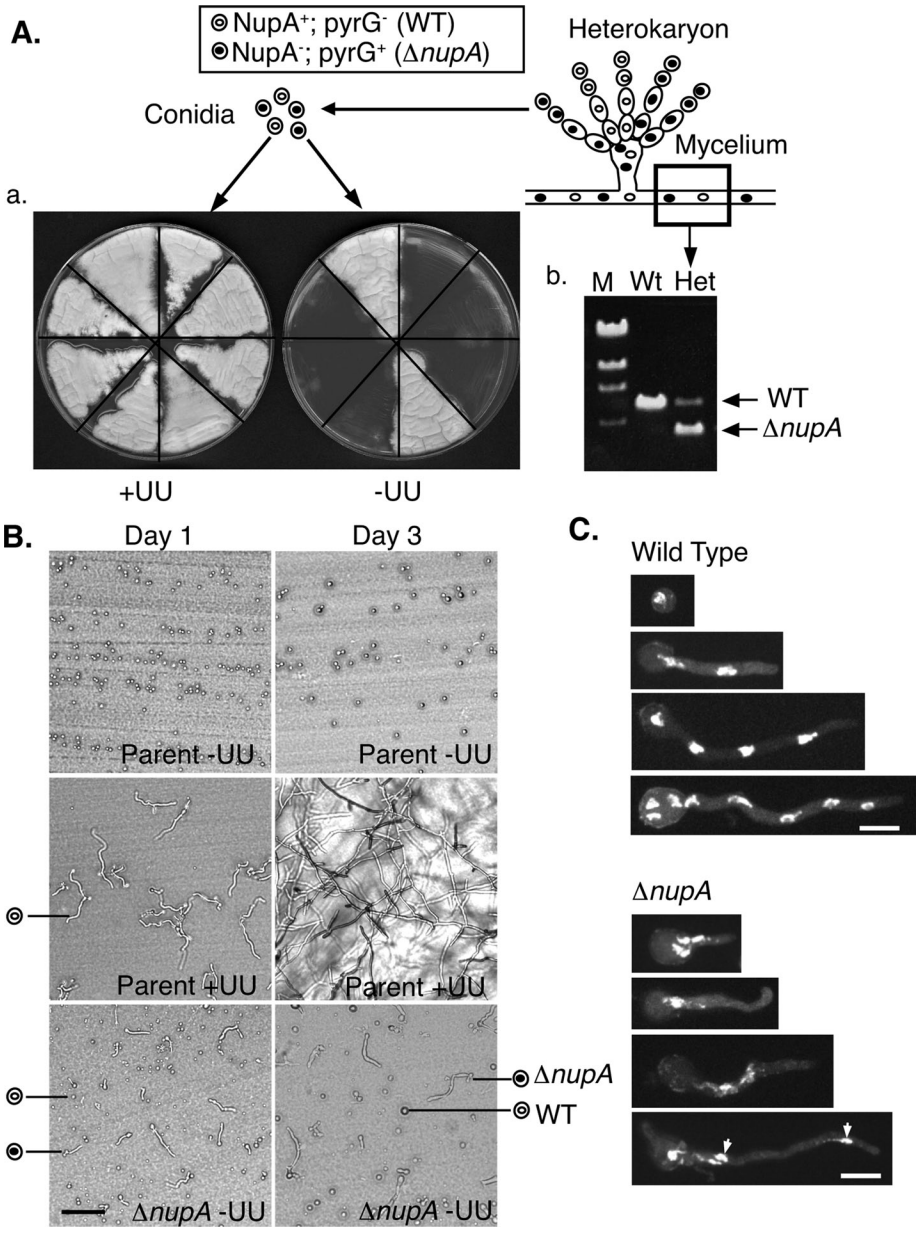

FIGURE 3: NupA is essential and its deletion, similar to Nup2, does not affect initial short-term growth but causes mitotic DNA segregation defects. (A) a, Conidia from Δ*nupA*::*pyrG* transformant colonies were streaked on media supplemented with or without uridine and uracil (UU). Because *nupA* is essential, heterokaryons were generated after transformation that contained parental nuclei and nuclei carrying Δ*nupA*::*pyrG*. The heterokaryotic colonies produce uninucleated spores able to form colonies on +UU (parental spores can form colonies) but not on –UU (neither parental nor Δ*nupA*::*pyrG* spores can form colonies). b, Diagnostic PCR of heterokaryon SM51 showing two bands corresponding to the wild-type *nupA* and the Δ*nupA*::*pyrG* allele. (B) Bright-field images of germinated spores from the parental strain or heterokaryon SM51 producing wild-type and Δ*nupA* spores grown for 1 or 3 d at 22°C on the indicated media. Bar, ~20 µm. (C) DAPI-stained wild-type germlings with typical one, two, four, and eight nuclei compared with Δ*nupA* germlings from heterokaryon SM51 of approximately the same length that had missegregated clustered DNA (arrows). Bar, ~5 µm.

(see below), it is possible that one could be responsible for the function of the other by targeting it correctly. To investigate this possibility, we deleted Nup2 in cells carrying NupA-GFP. In the absence of Nup2, NupA-GFP was able to locate to NPCs during interphase and to the chromatin region during mitosis (Figure 5B). In contrast, when *nupA* was deleted, Nup2-GFP was unable to locate to NPCs or to the mitotic chromatin region (Figure 5A). NupA is therefore required for Nup2 to locate to both interphase NPCs and the mitotic chromatin region.

Deletion of Nup2 or NupA causes mitotic defects that engage the spindle assembly checkpoint and also cause defects in karyokinesis

To investigate mitotic progression without Nup2 or NupA, we used GFP-tagged tubulin to monitor the dynamics of spindle formation (Ovechkina *et al.*, 2003). We found that the time to complete mitosis was longer and overall more variable in *nup2*- and *nupA*-deleted cells, taking 10–11 min on average to complete versus 5.5 min for wild-type cells (Figure 6, A and B, and Supplemental Figure S3). To see whether the mitotic defects caused by the absence of Nup2 and NupA are monitored by the SAC, we asked whether the mitotic delays in these mutants are dependent on a functional SAC response (Li and Murray, 1991; Musacchio and Salmon, 2007). We found that in the absence of Mad2, the mitotic delays caused by *nup2* or *nupA* deletion were abolished, and the average time of mitosis was similar to that of wild-type controls, with the variability in the duration of mitosis no longer apparent (Figure 6, A and B, and Supplemental Figure S3). We also followed Mad1-GFP in *nup2*- and *nupA*-null mutants to monitor SAC activation, which causes the transition of Mad1-GFP from NPCs to mitotic kinetochores. As occurs in the wild type, in the mutant Mad1-GFP translocates to kinetochores during the first mitosis during spore germination. Mad1-GFP then stays associated with the kinetochore region, as defined by Ndc80-ChRFP, during the extended mitotic period (Figure 6C). Absence of Nup2 or NupA therefore causes defects in mitosis, which are monitored by the SAC.

In cells lacking Nup2 or NupA, although the SAC is engaged causing mitotic delay, the cells do not all subsequently complete mitosis normally, even though the SAC is apparently fulfilled to allow progression into anaphase. This was revealed by monitoring formation of daughter nuclei in Δ*nupA* cells using the inner nuclear membrane (INM) marker AN0162-GFP in combination with NLS-DsRed. AN0162 is an INM marker that contains a C-terminal transmembrane domain and is similar to the *Schizosaccharomyces pombe* INM protein Bqt4 (unpublished data and annotated at AspGD as AN0162). During karyokinesis, the NE undergoes double restrictions and abscissions to generate daughter nuclei. This process also separates the nucleolus from nuclei (Ukil *et al.*, 2009). Twenty percent of *nupA*-null nuclei displayed defects during mitotic exit, and although two apparently normal G1 nuclei were initially formed, they

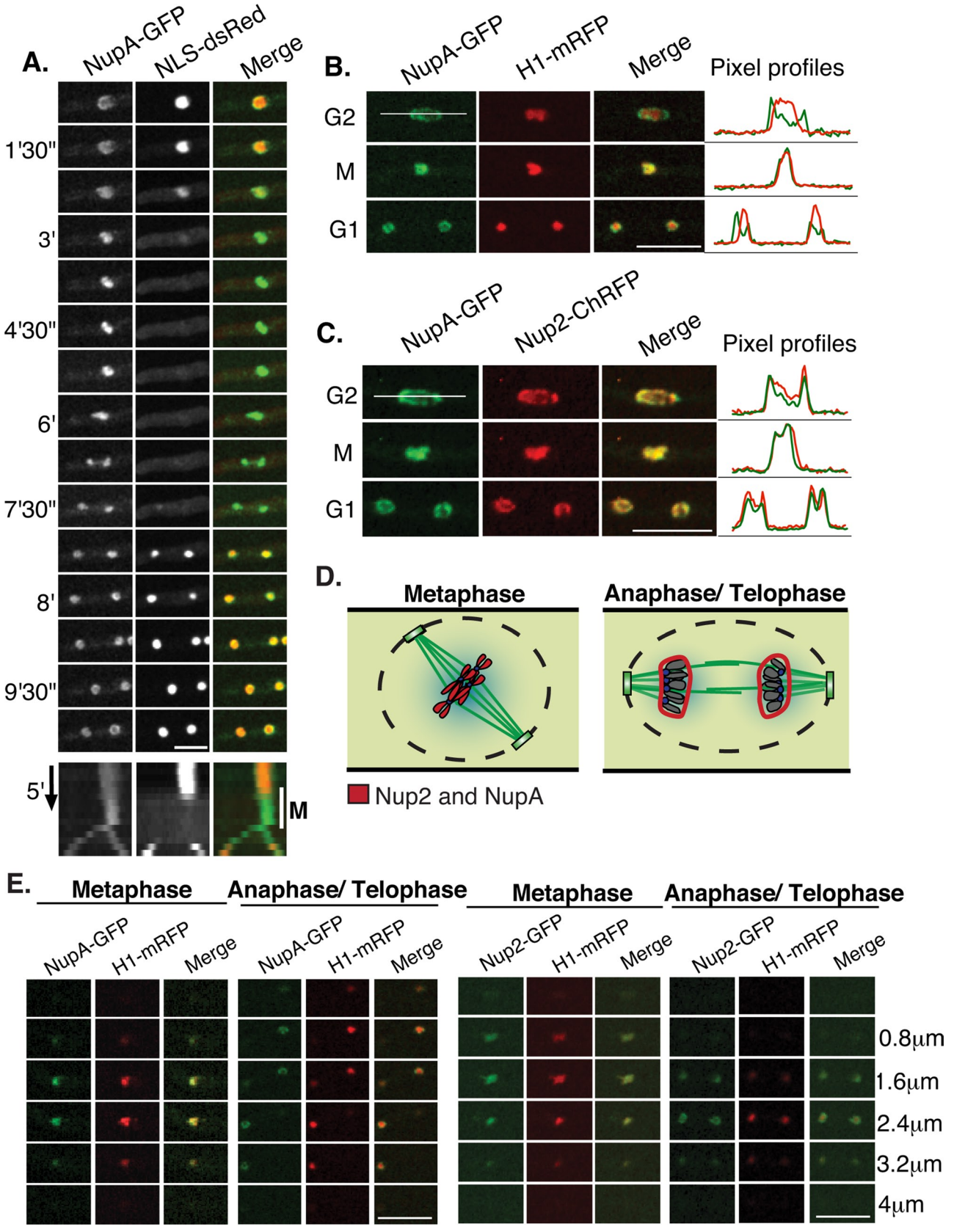

FIGURE 4: NupA localizes like Nup2 to NPCs during interphase and to the chromatin region during mitosis. (A) Images and kymograph from time-lapse microscopy (strain SM86) monitoring NupA-GFP and NLS-DsRed. NupA-GFP locates to the chromatin region during mitosis (M) as NLS-DsRed disperses from the mitotic nucleus when NPCs are partially disassembled. During exit from mitosis, NupA relocates back to NPCs as nuclear transport is reestablished. (B) NupA-GFP and Histone H1-mRFP in strain SM122 during G2, mitosis (M), and G1. Also shown are a merged image

and pixel profiles for both signals through the dividing nucleus. (C) NupA-GFP and Nup2-ChRFP in strain SM88 during G2, mitosis (M), and G1. Also shown are a merged image and pixel profiles for both signals through the dividing nucleus. (D) Cartoon of the location of Nup2 and NupA (red) during mitotic phases. (E) Sequential *z*-stack confocal images of Nup2-GFP and NupA-GFP in combination with Histone H1-mRFP in metaphase and anaphase/telophase as indicated (strains SO572 and SM124, respectively). Nuclei that had just exited metaphase and had their DNA still condensed were classified as anaphase–telophase. Nup2 and NupA move from throughout the chromatin region to around segregating chromatin after anaphase. Bar, ~5 µm.

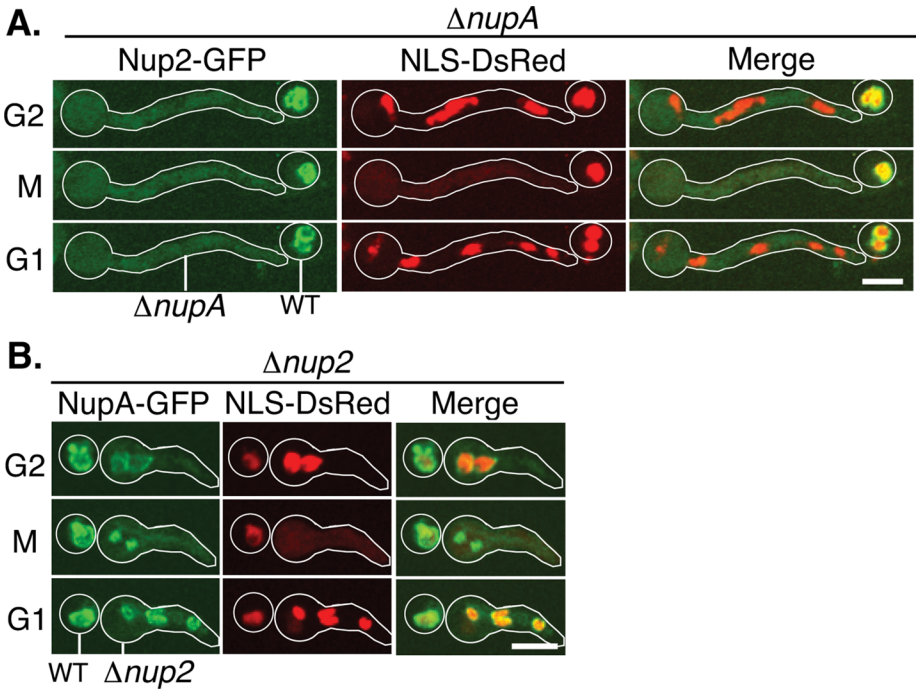

FIGURE 5: NupA is required for Nup2 location to interphase NPCs and to the mitotic chromatin region. (A, B) Time-lapse images of Nup2-GFP or NupA-GFP and NLS-DsRed and a merge in Δ*nupA* (from heterokaryon SM79) and Δ*nup2* (from heterokaryon SM92) germlings, respectively, (outlined in white) in G2, M (mitosis), and G1. Also outlined are parental spores within the same field of view that cannot germinate in the selective media used. (A) In the absence of NupA, Nup2 can locate to neither interphase NPCs nor the mitotic chromatin region. (B) Conversely, in the absence of Nup2, NupA can still locate to interphase NPCs and the mitotic chromatin region. Bar, ~5 µm.

remain associated via the NE, and karyokinesis failed, resulting in the formation of a single diploid nucleus (Figure 7, B and E). During failed nucleokinesis, AN0162 did not locate correctly around the nucleolus (compare Figure 7, A and B, arrow). Furthermore, after several rounds of mitosis, some mutant polyploid nuclei were seen to form multiple bipolar spindles during mitosis (Figure 7D), indicating that these nuclei were the products of more than one round of defective karyokinesis. Lack of Nup2 or NupA therefore compromises aspects of mitosis that are monitored by the SAC and also perturbs NE dynamics during mitotic exit, which can lead to failed karyokinesis.

Nup2 and NupA are not required for assembly of transport-competent NPCs but are required for Mad1 location to nuclei in G1

Nup2 and its mammalian orthologue Nup50 facilitate importin-α/β–mediated nuclear transport (Solsbacher *et al.*, 2000; Gilchrist *et al.*, 2002; Lindsay *et al.*, 2002; Matsuura and Stewart, 2005; Stewart, 2007; Makise *et al.*, 2012). Consistent with *A. nidulans* Nup2 playing a similar role, it purified with importins α and β (Figure 1C). To investigate their roles in nuclear transport, we monitored NLS-DsRed to detect whether Δ*nup2* and Δ*nupA* mutant nuclei are defective in nuclear protein import. NLS-DsRed was transported into Δ*nup2* and Δ*nupA* nuclei during interphase, with little to no cytoplasmic signal apparent (Figure 8, A and B, 0′). This indicates that nuclear transport is active in the absence of Nup2 or NupA. To determine whether the rate of NLS-DsRed nuclear transport is modified without Nup2 and NupA, we followed the rate of dispersal of NLS-DsRed during mitotic entry and then its rate of import during mitotic exit. As cells entered mitosis, NLS-DsRed dispersed from nuclei and was rapidly transported back into daughter G1 nuclei during mitotic exit in wild-type as well as Δ*nup2* and Δ*nupA* nuclei (Figure 8B). Note that NLS-DsRed remained mitotically dispersed longer in the mutants than the wild type because they have prolonged SAC-mediated delayed mitosis (Figure 6, A and B, and Supplemental Figure S3). We quantified the fluorescence pixel intensity of the nuclear NLS-DsRed signal at 10-s intervals in comparison to wild type (Figure 8C). Dispersal and import rates of NLS-DsRed in the mutants were comparable to wild type, with the kinetics of both being essentially superimposable between the mutants and wild type. This suggests there are no overall defects in nuclear protein import in the absence of Nup2 or NupA. In addition, because the disassembly and reassembly of NPCs drive release and reimport of NLS-DsRed, respectively, the results further indicate that the rates of mitotic NPC disassembly and reassembly are not affected by the absence of Nup2 or NupA.

Although transport of NLS-DsRed does not require Nup2 and NupA, we observed defects in the location of Mad1-GFP to nuclei after mitosis. Mad1-GFP displays distinct sequential cell cycle–regulated locations; NPCs during interphase, at kinetochores and the Mlp1-associated spindle matrix region during mitosis, transiently dispersed from nuclei during exit from mitosis and then briefly in the nucleoplasm before being reassembled back to NPCs in G1 (De Souza *et al.*, 2009; Figure 9A). In the absence of Nup2 or NupA, live-cell imaging revealed that Mad1-GFP located normally at NPCs before mitosis and also transitioned to kinetochores upon entry into mitosis, as expected (Figures 6C and 9A). Also as in wild-type cells, Mad1-GFP dispersed from nuclei during mitotic exit. However, in the absence of Nup2, Mad1-GFP failed to accumulate back into G1 nuclei normally after completion of mitosis (Figure 9A).

We analyzed the locations of Mad1-GFP in populations of wild-type, Δ*nup2*, and Δ*nupA* cells (Figure 9B). Because Mad1 locates to NPCs throughout most of interphase, the majority of wild-type cells contain Mad1-GFP at NPCs (Figure 9B). A smaller percentage of

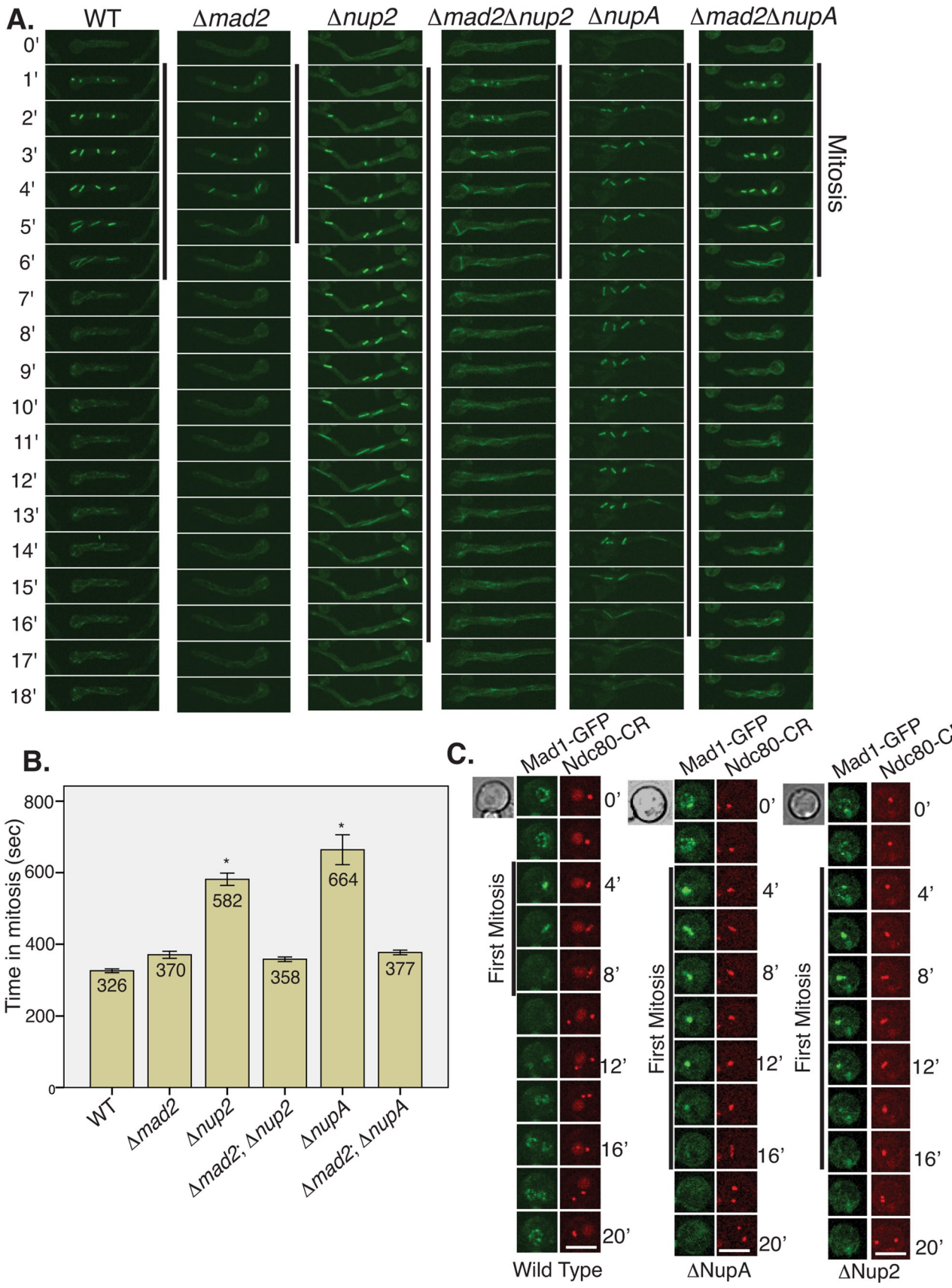

FIGURE 6: *nup2*- and *nupA*-deleted cells undergo delayed mitosis due to activation of the spindle assembly checkpoint. (A) Time course images of GFP-tubulin to follow mitotic spindle formation in germlings with four nuclei during G2-M-G1. Δ*nup2* (from heterokaryon SM96) and Δ*nupA* (from heterokaryon SM98) cells display a prolonged mitosis only when the SAC is functional. Bar, ~5 μm. (B) Bar graph representing average time spent in mitosis with mitotic spindles present for

each indicated genotype. The number on each bar represents the average time in seconds. Δ*nup2* and Δ*nupA* cells spend significantly longer time in mitosis than wild type (strain HA375) (with $p < 0.01$, highly significant when comparing the means). Δ*mad2* + Δ*nup2* (from heterokaryon SM129) and Δ*mad2* + Δ*nupA* (from heterokaryon SM131) mutants show no statistical difference compared with the wild type or Δ*mad2* mutant (strain CDS864). (C) Time course images of wild-type and *nupA*- and *nup2*-null cells during first mitosis following Mad1-GFP in combination with the kinetochore marker Ndc80-ChRFP in strain CDS831 and spores from heterokaryon SM154 and SM152, respectively. In the first mitosis of Δ*nupA* and Δ*nup2* nuclei, Mad1-GFP remains at kinetochores during the delayed mitosis. Bar, ~5 µm.

cells have Mad1-GFP located within nuclei at kinetochores, reflective of cells in mitosis (~5% of the cell cycle). An even smaller percentage of cells had Mad1-GFP dispersed from nuclei (Figure 9B), when it is transiently released from nuclei during mitotic exit before nuclear transport is reestablished during G1. In the absence of Nup2 or NupA, the percentage of cells with Mad1-GFP at the kinetochores remained largely unchanged (Figure 9B), indicating that Mad1's mitotic nuclear location, when nuclear pores are opened, does not require their functions. Of note, however, the low percentage of cells with Mad1-GFP dispersed was dramatically increased to ~50%, with a proportional decrease of cells with Mad1-GFP at NPCs (Figure 9B). Of importance, when the NPC tether for Mad1 is deleted (ΔMlp1), Mad1-GFP is effectively imported into interphase nuclei but cannot locate at NPCs (De Souza and Osmani, 2009). The fact that there is a dramatic increase in the number of cells in which Mad1-GFP remains cytoplasmic therefore indicates that without Nup2 or NupA, nuclear transport of Mad1-GFP is defective after mitosis rather than its ability to locate at NPCs. Because NLS-DsRed nuclear import is unaffected without NupA or Nup2, the nuclear import defect of Mad1 implies that they are required specifically for effective nuclear import of Mad1.

DISCUSSION

NupA is essential and was identified as a copurifying partner of Nup2 but contains no sequence characteristics of known NPC proteins and is poorly conserved even between *Aspergillus* species. NupA location was found to be regulated in an identical manner to Nup2 and to cause the same mitotic defects when deleted. Our analysis shows that NupA is required for the targeting of Nup2 to its interphase and mitotic locations and reveals Nup2 and NupA play interconnected roles during mitosis as well as during mitotic exit, being involved in transporting Mad1 to nuclei during G1 and also the control of karyokinesis.

Nup2 and NupA are required for aspects of mitosis as well as karyokinesis

During interphase, NupA and Nup2 locate around the nuclear periphery with NPCs, but at mitotic entry, they locate to the chromatin region within nuclei. Transition to the chromatin region depends upon mitotic activation of Cdk1, and both Nups are phosphorylated when located to the chromatin region. This adds these Nups to the growing number found to be phosphorylated in a mitotic-specific manner (Macaulay *et al.*, 1995; Favreau *et al.*, 1996; De Souza *et al.*, 2004; Mansfeld *et al.*, 2006; Glavy *et al.*, 2007; Blethrow *et al.*, 2008; Laurell *et al.*, 2011). The NIMA kinase, which is required and sufficient to promote NPC disassembly, is also able to promote the dissociation of Nup2 from NPCs and its transition to the chromatin region. Because Nup2 transition to the chromatin region at mitosis is conserved, as are the mitotic roles of CDK1 and NIMA during mitotic NPC disassembly (Laurell *et al.*, 2011), it is possible that related kinases in other species will regulate mitotic association of Nup2 to the mitotic chromatin region as occurs in *A. nidulans*.

The location of Nup2 and NupA first throughout the chromatin region during prophase and then around chromatin during anaphase and telophase suggests they could play roles during both early and late stages of mitosis. We show that their early mitotic roles, when they are located throughout the chromatin region, are monitored by the SAC, which is activated and engaged longer in their absence. In addition, without Nup2 or NupA function, and after apparent satisfaction of the SAC, a high percentage of mitoses failed karyokinesis, which generated polyploid nuclei. This phenotype suggests that their telophase locations around segregating genomes could also be of functional relevance, perhaps to help drive the double NE abscissions during karyokinesis. Arguing against a specific role for Nup2 and NupA in the mechanics of karyokinesis, many different mitotic defects have been shown to generate polyploid nuclei in *A. nidulans* (Enos and Morris, 1990; O'Connell *et al.*, 1993; De Souza *et al.*, 1999, 2011; De Souza and Osmani, 2011; Davies *et al.*, 2004; Pitt *et al.*, 2004; Prigozhina *et al.*, 2004; Govindaraghavan *et al.*, 2014). Because karyokinesis is aborted in response to many different mitotic defects in *A. nidulans*, we suggest that a regulatory mechanism is triggered, preventing completion of karyokinesis in response to postanaphase defects. We tentatively call this the karyokinesis checkpoint, although we have not formally proven that checkpoint-type regulation (Hartwell and Weinert, 1989) is in play. The karyokinesis checkpoint would prevent generation of aneuploid nuclei and generate polyploid nuclei instead. We observed polyploid nuclei generated in the absence of Nup2 or NupA form multiple bipolar spindles in a process akin to depolyploidization (Puig *et al.*, 2008; Lee *et al.*, 2009). Polyploid nuclei generated via the karyokinesis checkpoint can therefore contribute to cell growth and could also potentially undergo reductional mitotic division to regenerate correct ploidy, as previously seen after microtubule poison washout in *A. nidulans* (De Souza *et al.*, 2011).

The karyokinesis checkpoint has similarities with the Aurora B–mediated abscission checkpoint (NoCut pathway in budding yeast), which prevents aneuploidy by causing delays in cytokinesis if chromatin becomes trapped between daughter cells (Norden *et al.*, 2006; Chen and Doxsey, 2009; Steigemann and Gerlich, 2009; Steigemann *et al.*, 2009). However, in the early stages of *A. nidulans* growth, cytokinesis is not linked to mitosis (Clutterbuck, 1970; Harris *et al.*, 1994), and so cytokinesis cannot be a target of checkpoints involved in maintaining ploidy when mitotic DNA is slow to segregate. Instead, we propose that the final stage of NE abscission during nucleokinesis is the target of the regulatory mechanisms preventing generation of aneuploid nuclei after DNA segregation defects rather than cytokinesis in *A. nidulans*. In mammalian cells, delayed cytokinetic abscission can also be triggered when NPCs are not assembled correctly. This has been termed the NPC-abscission checkpoint (Mackay and Ullman, 2011). Of importance, the NPC-abscission checkpoint can be initiated by loss of Nup153 or Nup50 (Nup2 orthologue; Mackay *et al.*, 2010). Another checkpoint, active after the SAC, has recently been reported to act upon nuclear envelope reassembly and chromosome decondensation during mitotic exit (Afonso *et al.*, 2014). It will therefore be of interest to further investigate similarities and differences between the karyokinesis checkpoint of *A. nidulans* and those active in other cell types that ensure normal ploidy after defective mitosis.

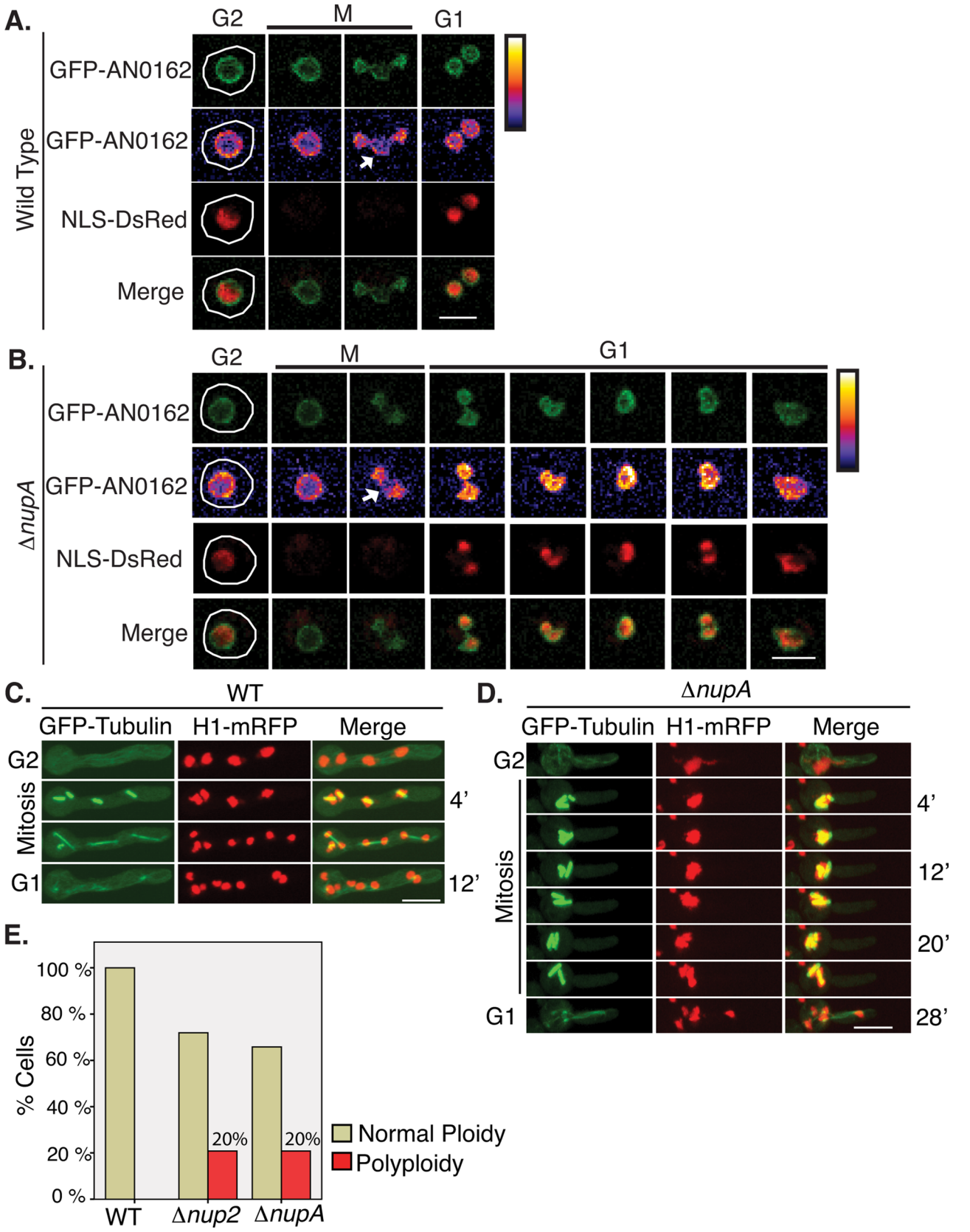

FIGURE 7: *nup2*- and *nupA*-null mutants display defects in mitotic exit. (A) Images captured during live-cell imaging of wild-type (SM116) and (B) *nupA*-null (Δ*nupA*, from heterokaryon SM127) strains during mitosis, monitoring the INM marker GFP-AN0162 and NLS-DsRed. Without NupA function, the nucleus fails to complete karyokinesis and forms one polyploid nucleus after mitosis. GFP-AN0162 does not locate to the periphery of the nucleolus after anaphase as obviously as the wild type (compare structures at arrows). Pseudocoloring represents false coloring using the thermal

color scale of ImageJ. The Fire Color lookup table was applied to grayscale images to produce false-color images (pixels with a value of 0 are white, and pixels with a value of 255 are black). Bar, ~2.5 µm. (C) Mitosis of a wild type (strain HA375) following spindle and chromatin dynamics of four mitotic nuclei. Bar, ~5 µm. (D) A mitotic depolyploidization event in a *nupA*-null mutant (from heterokaryon SM98) showing multiple bipolar spindles forming in a polyploid nucleus that remains in an extended metaphase-like state before exiting mitosis. Bar, ~5 µm. (E) Quantitation of the percentage of larger polyploid nuclei generated in wild-type (strain HA375) compared with *nup2*- and *nupA*-null cells (heterokaryons SM96 and SM98, respectively).

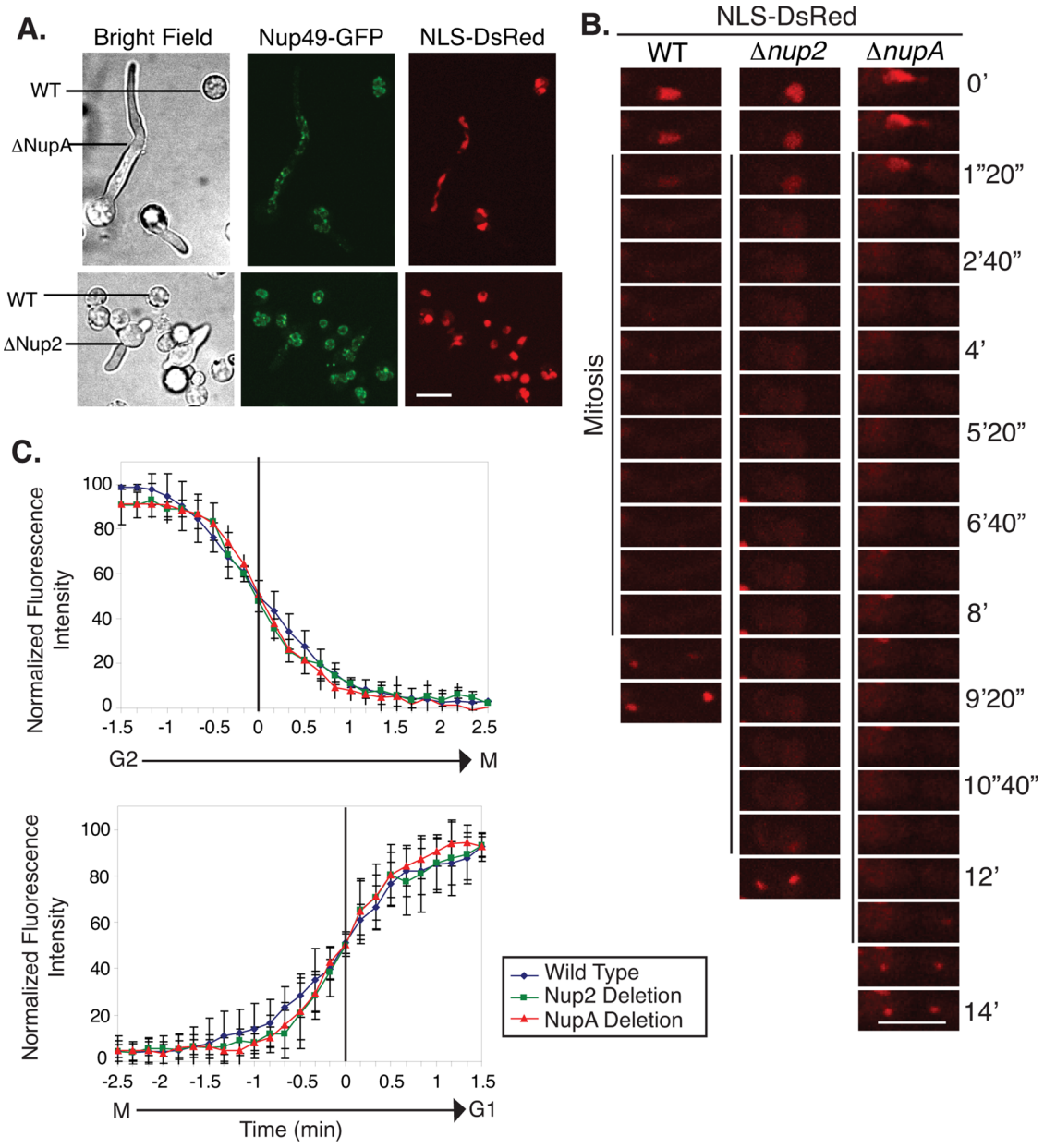

FIGURE 8: Nup2 and NupA are dispensable for nuclear NLS-DsRed nuclear import. (A) NLS-dsRed is actively imported to the nucleoplasm in Δ*nup2* and Δ*nupA* nuclei. Bright-field and confocal images of Δ*nupA* or Δ*nup2* germinated spores from heterokaryons SM117 and SM118, respectively, and wild-type spores grown on selective media. Bar, ~5 µm. (B) Time course images of NLS-DsRed nuclear dispersal and import during mitosis of wild-type (strain SM112), Δ*nup2* (from heterokaryon SM118), and Δ*nupA* (from heterokaryon SM117) cells. Bar, ~5 µm. (C) Rate of mitotic entry dispersal and mitotic exit import of NLS-DsRed in wild-type, Δ*nup2*, and Δ*nupA* cells, showing average normalized nuclear pixel intensity vs. time ($N = 10$; error bars ± SD). The pixel intensity of the red signal was quantified in a defined area within the nucleus every 10 s and the highest pixel intensity normalized to 100%. Time 0 represents the time at which 50% loss during mitotic entry, or gain during mitotic exit, of the normalized fluorescence intensity of the NLS-DsRed signal occurred.

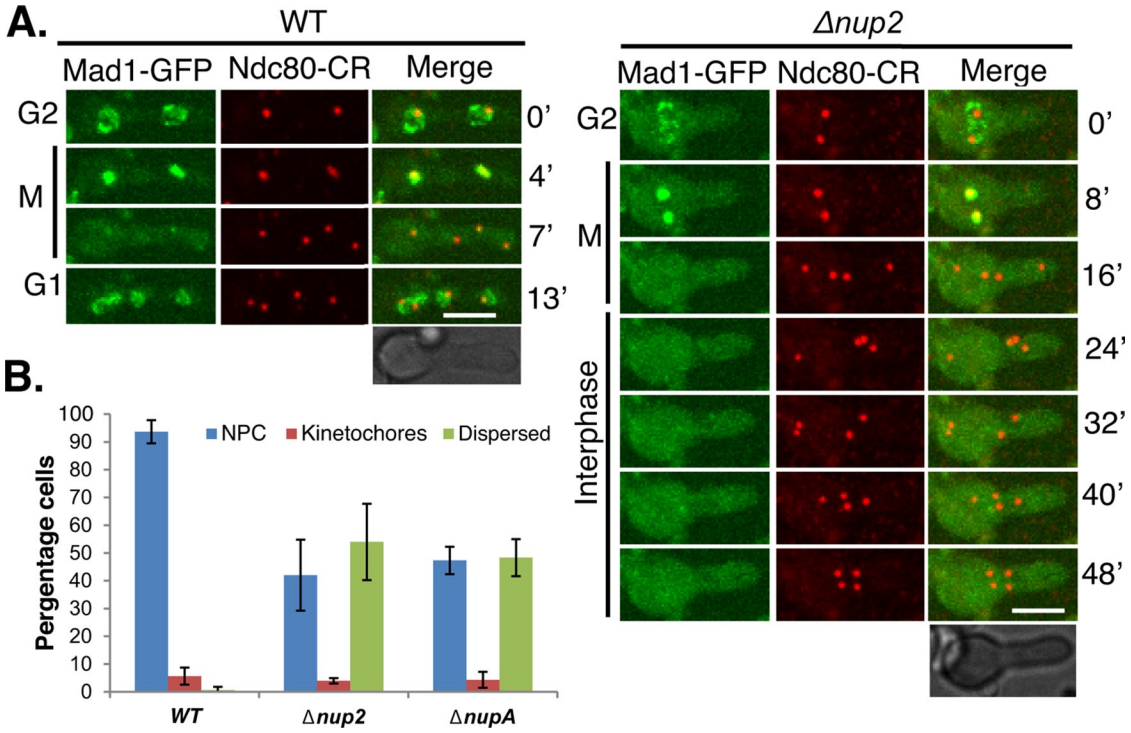

FIGURE 9: Nup2 and NupA affect the postmitotic nuclear import of Mad1. (A) Time-lapse microscopy of Mad1-GFP and the kinetochore marker Ndc80-ChRFP in wild-type (strain CDS578) and Δ*nup2* cells (heterokaryon SM152), showing that in the absence of Nup2, the mitotic location of Mad1 to kinetochores remains unaffected, but the nuclear import of Mad1 in G1 is impaired. Bar, ~5 μm. (B) Quantification of the mislocalization of Mad1 in asynchronously growing wild-type, Δ*nup2*, and Δ*nupA* cells.

Nup2 and NupA are not required for assembly of transport-competent NPCs but are required for Mad1 nuclear import

Nup2 and NupA are not required for nuclear import of NLS-DsRed, indicating that NPCs can functionally assemble without them, but they are involved in the interphase import of Mad1. The delayed nuclear import of Mad1 in the absence of Nup2 or NupA suggests they may facilitate Mad1 import. Nuclear protein import dependent upon specific Nups was previously defined for the Gag protein of the Tf1 retrotransposon of *S. pombe*, which requires Nup124 for its import. Nup124 is the *S. pombe* orthologue of Nup153 (Balasundaram *et al.*, 1999). Of importance, sequences adjacent to the Tf1 Gag NLS are sufficient to cause the classical NLS of SV40 to become dependent upon Nup124 for its nuclear import (Dang and Levin, 2000; Kim *et al.*, 2005; Varadarajan *et al.*, 2005; Sistla *et al.*, 2007). If similar functional sequences were associated with the NLSs of Mad1, this could explain the specific requirement for Nup2 and NupA for its nuclear import via the classical importin-α/β pathway.

Could NupA be a very poorly conserved functional equivalent to Nup153?

Although NupA does not contain sequence similarities to other Nups, indicating that it is a unique Nup, the results of our NupA studies reveal distinct parallels to findings from several systems for Nup153 and its orthologues, which include Nup1 and Nup60 in *S. cerevisiae* and Nup124 in *S. pombe*. They interact and purify with the same proteins, including Nup2 and importins α and β (Guan *et al.*, 2000; Smitherman *et al.*, 2000; Allen *et al.*, 2001, 2002; Denning *et al.*, 2001; Dilworth *et al.*, 2001, 2005; Sistla *et al.*, 2007), are required for formation of the nuclear basket complex (Denning *et al.*, 2001; Dilworth *et al.*, 2001; Hase and Cordes, 2003), play roles in aspects of mitosis before and after the SAC response (Mackay *et al.*, 2009, 2010; Mackay and Ullman, 2011; Lussi *et al.*, 2010), and are poorly conserved even between closely related species (Mans *et al.*, 2004; Bapteste *et al.*, 2005; Sistla *et al.*, 2007). Given that the Nup153 equivalent in *S. pombe* is required for nuclear import and activity of the retrotransposon Tf1 (Varadarajan *et al.*, 2005), one driving force promoting the rapid variance in Nup153-related proteins, potentially including NupA, could be the result of an ongoing arms race between viruses/retrotransposons and their host cells that involves Nup153-related proteins.

MATERIALS AND METHODS

General techniques

General techniques for classical genetics, media preparation, and culture of *A. nidulans* were as previously described (Pontecorvo *et al.*, 1953; Osmani *et al.*, 2006a). *A. nidulans* transformation was conducted as described (Osmani *et al.*, 1987), but 10 mg/ml Vinoflow FCE (Novozymes A/S, Bagsvaerd, Denmark) was used instead of Novozyme 234 in the lytic mix. 4′,6-Diamidino-2-phenylindole (DAPI) staining of DNA was performed as described (Oakley and Osmani, 1993). Genes were endogenously tagged at their 3′ end using constructs generated by fusion PCR as described (Yang *et al.*, 2004; Szewczyk *et al.*, 2006) and transformed into an *nku*A^{ku70}Δ strain (SO451) (Nayak *et al.*, 2006). DNA was prepared from these strains as described (Osmani *et al.*, 2006a), and diagnostic PCR using primers flanking the targeting construct was performed to verify homologous integration. Haploid strains used in this study are listed in Table 1. Protein was extracted from *A. nidulans* as described (Osmani *et al.*, 2006a; Liu *et al.*, 2010), and Western blotting analysis was performed (Osmani *et al.*, 2006a) to confirm correct expression

Strain	Genotype	Reference
R153	*wA3; pyroA4*	De Souza *et al.* (2004)
SO451	*wA3; chaA1; fwA1; pyroA4; pyrG89; argB2; nkuA^{ku70}Δ::argB; SE15; nirA14*	Osmani *et al.* (2006a)
SO926	*An-nup2-S-Tag::pyrG^{Af}; pyrG89; nimT23; pyroA4; yA2; nirA14?*	This study
CDS831	*ndc80-ChRFP::pyroA^{Af}; mad1-GFP::pyro^{Af}; ΔnkuA^{ku70}::argB; pyroA4; pyrG89; argB2; chaA1; wA3; nirA14?; fwA1?*	De Souza *et al.* (2009)
SO572	*An-nup2-GFP::pyrG; pyrG89; H1-mRFP; pabaA1; wA3*	This study
CDS864	*Δmd2A::pyroA^{Af}; nup49-ChRFP::pyroA^{Af}; GFP-TubA; pyrG89; argB2; ΔnKuA^{Ku70}::argB; fwA1; chaA1; pyroA4?; nirA14?*	This study
HA375	*nimT23; tubA-GFP; An-H1-ChRFP::pyroA^{Af}; pyrG89; pyroA4; argB2?; ΔnkuA^{ku70}::argB*	This study
HA377	*nimT23; An-Nup2-GFP::pyroA^{Af}; ΔyA::NLS-Dsred-StuA; pyrG89; pyroA4; argB2?; ΔnkuAku70::argB*	This study
SO1030	*alcA-nimA-ΔC S-tag::pyr4; pyrG89; An-nup2-GFP::pyroA^{Af}; pyroA4; ΔnKuA::argB alcA; argB2?; ΔyA::nlsdsRed; nimT23; yA2.*	This study
SM86	*nupA-GFP::pyroA; nimT23; pyrG89; pyroA4; argB2; ΔnkuA^{ku70}::argB; ΔyA::NLS-Dsred-StuA*	This study
SM88	*nupA-GFP::loxp2-pyrG^{Af}; pyrG89; nup2-ChRFP-pyroA^{Af}; pyroA4; wA3; chaA1; fwA1*	This study
SM112	*pyrG89; nimT23; pyroA4; An-nup49-GFP::riboB^{Af}; ΔnkuAku70::argB; ΔyA::NLS-DsRed-StuA; riboB2?; argB2?*	This study
SM116	*pyrG89; pyroA4; nirA14; pabaA1; ΔnkuAku70::argB; argB2?; ΔyA::NLS-DsRed-StuA; GFP-An0162*	This study
SM122	*H1-mRFP::pyrG^{Af}; pyrG89; nupA-GFP::loxp; argB2; nirA14?*	This study
SM124	*H1-mRFP::pyrG^{AF}; pyrG89; NupA GFP:: loxp; pyroA4; chA1*	This study
CDS578	*mad1-GFP::pyrG^{Af}; Ndc80-ChRFP::pyrG^{Af}; pyrG89; argB2; chaA1; fwA1; nirA14?*	De Souza *et al.* (2009)

In some strains, we have not confirmed some nutritional or color markers that could be covered by, or be recessive to, other markers in the strain (these are designated by a question mark).

^{Af} Genes from *A. fumigatus* used for complementation of the corresponding *A. nidulans* nutritional mutations.

TABLE 1: *A. nidulans* haploid strains used in this study.

Strain	Genotype	Parent
SM51	*wA3; fwA1; chaA1?; ΔnupA::pyrG^{Af}; pyrG89; ΔnkuA^{ku70}::argB; argB2; pyroA4; nirA14; sE15*	SO451
SM79	*ΔnupA::pyrG^{AF}; An-nup2-GFP::pyroA^{Af}; nimT23; ΔyA::NLS-Dsred-StuA; pyrG89; pyroA4; argB2?; ΔnkuA^{ku70}::argB*	HA377
SM92	*Δnup2::pyrG^{Af}; nupA-GFP::pyroA; nimT23; pyrG89; pyroA4; ΔnkuA^{ku70}::argB; ΔyA::NLS-DsRed-StuA*	SM86
SM96	*Δnup2::pyrG^{Af}; nimT23; GFP-tubA; An-H1-ChRFP::pyroA^{Af}; pyrG89; pyroA4; argB2?; nkuA^{ku70}Δ::argB*	HA375
SM98	*ΔnupA::pyrG^{Af}; nimT23; GFP-tubA; An-H1-ChRFP::pyroA^{Af}; pyrG89; pyroA4; argB2?; ΔnkuA^{ku70}::argB*	HA375
SM117	*ΔnupA::pyrG^{Af}; pyrG89; nimT23; pyroA4; An-Nup49-GFP::riboB^{Af}; ΔnkuA^{ku70}::argB; ΔyA::NLS-DsRed-StuA; riboB2?; argB2?*	SM112
SM118	*Δnup2::pyrG^{Af}; pyrG89; nimT23; pyroA4; An-nup49-GFP::riboB^{Af}; ΔnkuA^{ku70}::argB; ΔyA::NLS-DsRed-StuA; riboB2?; argB2?*	SM112
SM127	*ΔnupA::pyrG^{Af}; pyrG89; pyroA4; nirA14; pabaA1; ΔnkuA^{ku70}::argB; argB2?; ΔyA::NLS-DsRed-StuA; GFP-An0162*	SM116
SM129	*Δnup2::pyrG^{Af}; Δmd2A::pyroA^{Af}; nup49-ChRFP::pyroA^{Af}; GFP-tubA; pyrG89; argB2; ΔnKuA^{Ku70}::argB; fwA1; chaA1; pyroA4?; nirA14?*	CDS864
SM131	*ΔnupA::pyrG^{Af}; Δmd2A::pyroA^{Af}; nup49-ChRFP::pyroA^{Af}; GFP-tubA; pyrG89; argB2; ΔnKuA^{Ku70}::argB; fwA1; chaA1; pyroA4?; nirA14?*	CDS864
SM152	*Δnup2::pyrG^{Af}; ndc80-ChRFP::pyroA^{Af}; mad1-GFP::pyro^{Af}; ΔnkuA ^{ku70}::argB; pyroA4; pyrG89; argB2; chaA1; wA3; nirA14?; fwA1?*	CDS831
SM154	*ΔnupA::pyrG^{Af}; ndc80-ChRFP::pyroA^{Af}; mad1-GFP::pyro^{Af}; ΔnkuA ^{ku70}::argB; pyroA4; pyrG89; argB2; chaA1; wA3; nirA14?; fwA1?*	CDS831

The parent strain represents the strain in which the deletion or replacement of either *nup2* or *nupA* was performed. In some strains, we have not confirmed all nutritional or color markers that could be covered by, or be recessive to, other markers in the strain (these are designated by a question mark).

^{Af} Genes from *A. fumigatus* used for complementation of the corresponding *A. nidulans* nutritional mutations.

TABLE 2: *A. nidulans* heterokaryons used in this study.

and the specificity of the Nup2 antibody generated. The heterokaryon rescue technique was performed as described previously (Osmani *et al.*, 2006b), and heterokaryons used in this study are listed in Table 2.

Antibody generation and immunofluorescence

A rabbit polyclonal antibody was generated against the 874- to 1074-aa region of *A. nidulans* Nup2 cloned into Pet14b

(Novagen, Merck KGaA, Darmstadt, Germany) expressed and purified from *Escherichia coli* strain BL21 (DE3). Purified Nup2 was used to immunize male rabbits, and affinity-purified antibodies were produced by Bethyl Laboratories (Montgomery, TX). Immunofluorescence was performed (Oakley and Osmani, 1993) with some modifications. Cells were grown on yeast extract media and fixed in 1× PHEM buffer (45 mM 1,4-piperazinediethanesulfonic acid, 45 mM 4-(2-hydroxyethyl)-1-piperazineethanesulfonic acid, 10 mM ethylene glycol tetraacetic acid, 5 mM MgCl, pH 6.9) containing 6% paraformaldehyde (EM grade; Electron Microscopy Sciences, Hatfield, PA). Cell wall removal solution contained 10 mg/ml Vinoflow FCE (Novozymes A/S). Cells were digested for 50 min at 30°C. The antibody was used at a dilution of 1:5000.

Affinity purification and mass spectrometry

The S-tag affinity purification of endogenously S-tagged proteins was as described in Liu *et al.* (2009). G2 and M samples were generated by arresting cells in G2 using the *nimT23* temperature-sensitive mutation, which prevents activation of mitotic Cdk1, and then releasing to permissive temperature after addition of benomyl to cause synchronous mitotic SAC arrest (Osmani *et al.*, 1991; O'Connell *et al.*, 1992; Lu *et al.*, 1993). Samples were run on 10% SDS–PAGE and fixed, and protein was visualized by Bio-Safe Coomassie (Bio-Rad, Hercules, CA). Mass spectroscopy was completed at the Ohio State University Chemical Instrument Center. Phosphatase treatment was performed as described previously (De Souza *et al.*, 2004).

Sequencing and identification of NupA

cDNA and genomic DNA of NupA were amplified from *A. nidulans* cDNA libraries or genomic DNA. Pfu-turbo DNA polymerase (Stratagene, Santa Clara, CA) was used for high-fidelity amplification. The resulting PCR products were cloned in pCR 2.1-TOPO vector (Invitrogen, Carlsbad, CA) and sequenced. The 5′ and 3′ rapid amplification of cDNA ends was performed following the Marathon-Ready cDNA user manual (Clontech, Mountain View, CA) to confirm the N-terminal and C-terminal ends of *nupA*. To define the 5′ intron in *A. fumigatus nupA*, we PCR amplified the region that spans the intron using an *A. fumigatus* cDNA library (a kind gift from Gregory S. May, University of Texas MD Anderson Cancer Center, Houston, TX), which amplified a single band of a size predicted after intron splicing that was confirmed by sequence analysis.

NIMA induction experiments

Conidia from strains HA377 (wild type for NIMA) and SO1030 (*alcA*-NIMA-ΔC-Stag) were inoculated overnight in 1 l of minimal medium containing glucose at 26°C. Cultures were then centrifuged, washed twice with minimal media without carbon, and shifted into minimal medium containing 0.5% ethanol to induce NIMA expression. Mycelia samples were taken every 15 min. Extracted whole-cell protein samples from mycelia were run on SDS–PAGE. Western blot analysis was performed with NIMA antibody (F68) at a dilution of 1:2000 and the Nup2 antibody generated at a dilution of 1:5000. To follow Nup2-GFP by live-cell imaging, strains HA377 and SO1030 were grown overnight at room temperature in minimal medium containing glucose. The next day, the cells were either kept on minimal medium glucose for repressing conditions or washed twice with minimum medium without carbon and supplied with minimum medium containing 0.5% ethanol to induce NIMA expression. Hydroxyurea (20 mM) was used to arrest cells at S phase. After 2 h, Nup2-GFP and NLS-DsRed were followed in these cells as described in *Imaging and analysis*. Graphs were plotted depicting the cumulative number of cells that had Nup2 on DNA with time.

Imaging and analysis

Fixed samples were examined using an E800 microscope (Nikon, Melville, NY) with DAPI, fluorescein isothiocyanate , or Texas Red filters (Omega Optical, Brattleboro, VT). Image capture was performed using an UltraPix digital camera (Life Science Resources, Great Shelford, United Kingdom) and analyzed by Ultraview image capture software (PerkinElmer, Waltham, MA). For live-cell imaging, spores were germinated in 35-mm glass-bottom Petri dishes (MatTek Cultureware, Ashland, MA) in 3 ml of minimal medium containing 55 mM glucose as the carbon source and 10 mM urea as the nitrogen source at room temperature (21–23°C) for 24 h or until the 4- to 8-nucleus stage was reached. Spores from heterokaryons were germinated at room temperature (21–23°C) in YG medium (yeast extract glucose: 56 mM glucose, 5 g/l yeast extract, 10 mM magnesium sulfate, 1 μg/ml *p*-aminobenzoic acid, 0.5 μg/ml pyrodoxine HCl, 2.5 μg/ml riboflavin HCl, 2 μg/ml nicotinic acid, 20 μg/ml choline, 20 ng/ml D-biotin, and 1 ml/l trace elements) with or without uridine or uracil complementation for 8 h (to image first mitosis) or longer to image the second or third mitosis and terminal phenotypes. Visualization of GFP/ChRFP fusion proteins was performed using an inverted microscope (Nikon) configured with an Ultraview spinning disk confocal system and controlled by Ultraview software (PerkinElmer) utilizing Nikon Plan Apo 60×/numerical aperture 1.40 oil objectives. Image analysis, kymograph generation, and pixel intensity profiles were carried out using ImageJ (National Institutes of Health, Bethesda, MD). All images are represented as maximum-intensity projections as described (Ukil *et al.*, 2009).

Quantification of nuclear import

Cells were grown in YG with (for wild type) or without UU (for Δ*nup2* and Δ*nupA*) at room temperature (21–23°C) overnight and NLS-DsRed images captured every 10 s. Maximum pixel intensity (MPI) of *z*-sections spaced at 0.8 μm was measured using ImageJ. The normalized fluorescence intensity for each time point captured was measured as

$$\frac{\text{mean MPI of an area}(A)\text{(nucleus)} - \text{mean MPI of an identical-sized area}(A)\text{(cytoplasm)} \times 100}{\text{mean MPI of an identical-sized area}(A)\text{ with the highest mean MPI}}$$

Graphs were plotted using Excel (Microsoft, Redmond, WA) as normalized mean fluorescence intensity measured versus time (8–13 nuclei were measured for each genotype).

Quantification of time in mitosis

To calculate time spent in mitosis, cells were grown on YG with (for wild type, Δ*mad2*) or without UU (for Δ*nup2*, Δ*nupA,* Δ*nup2*Δ*mad2*, and Δ*nupA*Δ*mad2*) at room temperature (21–23°C) overnight (12–16 hr), and GFP-tubulin signal was followed throughout mitosis. Images were captured every 30 s using a spinning-disk confocal microscope (details described earlier). Time in mitosis was measured starting from the time point where the spindle is visible until it disassembled. Statistical analysis was conducted using PASW statistical software (SPSS, Chicago, IL). The *p* values were calculated using the Student's *t* test, considering $p < 0.05$ as significantly different with 95%

confidence intervals and p <0.01 as highly significant with 99% confidence.

Analysis of Mad1 dynamics without Nup2 and NupA function

For analysis of Mad1 localization in Δ*nup2* and Δ*nupA* null mutants, we used the heterokaryon rescue technique as described (Osmani *et al*., 2006b). Images of Δ*nup2* cells were captured after 24 h of growth, and the terminal phenotypes were analyzed and quantified. Δ*nup2*::*pyrG*^{Af} and Δ*nupA*::*pyrG*^{Af} cells in which Mad1-GFP signals were enriched at the nuclear periphery were classified as NPC location. When the signal was uniformly distributed throughout the cell with no particular enrichment, it was classified as dispersed. For Mad1-GFP localization analysis, cells were classified as kinetochores if Mad1-GFP colocalized with the kinetochore marker Ndc80-ChRFP.

ACKNOWLEDGMENTS

We thank all members of the Osmani laboratory, particularly Colin P.C. De Souza, for helpful discussions, critical reading of the manuscript, and strains CDS864, CDS578, and CDS831 and Hui-Lin Liu posthumously for strains HA375 and HA377. We thank John R. Davies for help in generating the Nup2 antibody and Jennifer Larson for critical reading of the manuscript. We thank Gregory S. May, University of Texas MD Anderson Cancer Center, for providing the *A. fumigatus* cDNA library. This work was supported by a grant from the National Institutes of Health (GM042564) to S.A.O.

REFERENCES

Afonso O, Matos I, Pereira AJ, Aguiar P, Lampson MA, Maiato H (2014). Feedback control of chromosome separation by a midzone Aurora B gradient. Science 345, 332–336.

Alber F, Dokudovskaya S, Veenhoff LM, Zhang W, Kipper J, Devos D, Suprapto A, Karni-Schmidt O, Williams R, Chait BT, *et al.* (2007). Determining the architectures of macromolecular assemblies. Nature 450, 683–694.

Allen NP, Huang L, Burlingame A, Rexach M (2001). Proteomic analysis of nucleoporin interacting proteins. J Biol Chem 276, 29268–29274.

Allen NP, Patel SS, Huang L, Chalkley RJ, Burlingame A, Lutzmann M, Hurt EC, Rexach M (2002). Deciphering networks of protein interactions at the nuclear pore complex. Mol Cell Proteomics 1, 930–946.

Arnaoutov A, Azuma Y, Ribbeck K, Joseph J, Boyarchuk Y, Karpova T, McNally J, Dasso M (2005). Crm1 is a mitotic effector of Ran-GTP in somatic cells. Nat Cell Biol 7, 626–632.

Balasundaram D, Benedik MJ, Morphew M, Dang VD, Levin HL (1999). Nup124p is a nuclear pore factor of *Schizosaccharomyces pombe* that is important for nuclear import and activity of retrotransposon Tf1. Mol Cell Biol 19, 5768–5784.

Bapteste E, Charlebois RL, MacLeod D, Brochier C (2005). The two tempos of nuclear pore complex evolution: highly adapting proteins in an ancient frozen structure. Genome Biol 6, R85.

Bayliss R, Littlewood T, Stewart M (2000). Structural basis for the interaction between FxFG nucleoporin repeats and importin-beta in nuclear trafficking. Cell 102, 99–108.

Belgareh N, Rabut G, Bai SW, van Overbeek M, Beaudouin J, Daigle N, Zatsepina OV, Pasteau F, Labas V, Fromont-Racine M, *et al.* (2001). An evolutionarily conserved NPC subcomplex, which redistributes in part to kinetochores in mammalian cells. J Cell Biol 154, 1147–1160.

Blethrow JD, Glavy JS, Morgan DO, Shokat KM (2008). Covalent capture of kinase-specific phosphopeptides reveals Cdk1-cyclin B substrates. Proc Natl Acad Sci USA 105, 1442–1447.

Blower MD, Nachury M, Heald R, Weis K (2005). A Rae1-containing ribonucleoprotein complex is required for mitotic spindle assembly. Cell 121, 223–234.

Bolhy S, Bouhlel I, Dultz E, Nayak T, Zuccolo M, Gatti X, Vallee R, Ellenberg J, Doye V (2011). A Nup133-dependent NPC-anchored network tethers centrosomes to the nuclear envelope in prophase. J Cell Biol 192, 855–871.

Booth JW, Belanger KD, Sannella MI, Davis LI (1999). The yeast nucleoporin Nup2p is involved in nuclear export of importin alpha/Srp1p. J Biol Chem 274, 32360–32367.

Buchwalter AL, Liang Y, Hetzer MW (2014). Nup50 is required for cell differentiation and exhibits transcription-dependent dynamics. Mol Biol Cell 25, 2472–2484.

Buffin E, Lefebvre C, Huang J, Gagou ME, Karess RE (2005). Recruitment of Mad2 to the kinetochore requires the Rod/Zw10 complex. Curr Biol 15, 856–861.

Campbell MS, Chan GK, Yen TJ (2001). Mitotic checkpoint proteins HsMAD1 and HsMAD2 are associated with nuclear pore complexes in interphase. J Cell Sci 114, 953–963.

Casolari JM, Brown CR, Komili S, West J, Hieronymus H, Silver PA (2004). Genome-wide localization of the nuclear transport machinery couples transcriptional status and nuclear organization. Cell 117, 427–439.

Chen CT, Doxsey S (2009). A last-minute rescue of trapped chromatin. Cell 136, 397–399.

Clutterbuck AJ (1970). Synchronous nuclear division and septation in *Aspergillus nidulans*. J Gen Microbiol 60, 133–135.

Cross MK, Powers MA (2011). Nup98 regulates bipolar spindle assembly through association with microtubules and opposition of MCAK. Mol Biol Cell 22, 661–672.

Dang VD, Levin HL (2000). Nuclear import of the retrotransposon Tf1 is governed by a nuclear localization signal that possesses a unique requirement for the FXFG nuclear pore factor Nup124p. Mol Cell Biol 20, 7798–7812.

D'Angelo MA, Hetzer MW (2008). Structure, dynamics and function of nuclear pore complexes. Trends Cell Biol 18, 456–466.

Davies JR, Osmani AH, De Souza CP, Bachewich C, Osmani SA (2004). Potential link between the NIMA mitotic kinase and nuclear membrane fission during mitotic exit in *Aspergillus nidulans*. Eukaryot Cell 3, 1433–1444.

De Souza CP, Hashmi SB, Nayak T, Oakley B, Osmani SA (2009). Mlp1 acts as a mitotic scaffold to spatially regulate spindle assembly checkpoint proteins in *Aspergillus nidulans*. Mol Biol Cell 20, 2146–2159.

De Souza CP, Hashmi SB, Yang X, Osmani SA (2011). Regulated inactivation of the spindle assembly checkpoint without functional mitotic spindles. EMBO J 30, 2648–2661.

De Souza CP, Osmani AH, Hashmi SB, Osmani SA (2004). Partial nuclear pore complex disassembly during closed mitosis in *Aspergillus nidulans*. Curr Biol 14, 1973–1984.

De Souza CP, Osmani SA (2007). Mitosis, not just open or closed. Eukaryot Cell 6, 1521–1527.

De Souza CP, Osmani SA (2009). Double duty for nuclear proteins—the price of more open forms of mitosis. Trends Genet 25, 545–554.

De Souza CP, Osmani SA (2011). A new level of spindle assembly checkpoint inactivation that functions without mitotic spindles. Cell Cycle 10, 3805–3806.

De Souza CP, Ye XS, Osmani SA (1999). Checkpoint defects leading to premature mitosis also cause endoreplication of DNA in *Aspergillus nidulans*. Mol Biol Cell 10, 3661–3674.

Denning D, Mykytka B, Allen NP, Huang L, Al B, Rexach M (2001). The nucleoporin Nup60p functions as a Gsp1p-GTP-sensitive tether for Nup2p at the nuclear pore complex. J Cell Biol 154, 937–950.

Denning DP, Uversky V, Patel SS, Fink AL, Rexach M (2002). The *Saccharomyces cerevisiae* nucleoporin Nup2p is a natively unfolded protein. J Biol Chem 277, 33447–33455.

Dilworth DJ, Suprapto A, Padovan JC, Chait BT, Wozniak RW, Rout MP, Aitchison JD (2001). Nup2p dynamically associates with the distal regions of the yeast nuclear pore complex. J Cell Biol 153, 1465–1478.

Dilworth DJ, Tackett AJ, Rogers RS, Yi EC, Christmas RH, Smith JJ, Siegel AF, Chait BT, Wozniak RW, Aitchison JD (2005). The mobile nucleoporin Nup2p and chromatin-bound Prp20p function in endogenous NPC-mediated transcriptional control. J Cell Biol 171, 955–965.

Ding D, Muthuswamy S, Meier I (2012). Functional interaction between the *Arabidopsis* orthologs of spindle assembly checkpoint proteins MAD1 and MAD2 and the nucleoporin NUA. Plant Mol Biol 79, 203–216.

Dultz E, Zanin E, Wurzenberger C, Braun M, Rabut G, Sironi L, Ellenberg J (2008). Systematic kinetic analysis of mitotic dis- and reassembly of the nuclear pore in living cells. J Cell Biol 180, 857–865.

Enos AP, Morris NR (1990). Mutation of a gene that encodes a kinesin-like protein blocks nuclear division in *A. nidulans*. Cell 60, 1019–1027.

Favreau C, Worman HJ, Wozniak RW, Frappier T, Courvalin JC (1996). Cell cycle-dependent phosphorylation of nucleoporins and nuclear pore membrane protein Gp210. Biochemistry 35, 8035–8044.

Frey S, Gorlich D (2007). A saturated FG-repeat hydrogel can reproduce the permeability properties of nuclear pore complexes. Cell 130, 512–523.
Frey S, Richter RP, Gorlich D (2006). FG-rich repeats of nuclear pore proteins form a three-dimensional meshwork with hydrogel-like properties. Science 314, 815–817.
Galagan JE, Calvo SE, Cuomo C, Ma LJ, Wortman JR, Batzoglou S, Lee SI, Basturkmen M, Spevak CC, Clutterbuck J, *et al.* (2005). Sequencing of *Aspergillus nidulans* and comparative analysis with A. fumigatus and A. oryzae. Nature 438, 1105–1115.
Galy V, Askjaer P, Franz C, Lopez-Iglesias C, Mattaj IW (2006). MEL-28, a novel nuclear-envelope and kinetochore protein essential for zygotic nuclear-envelope assembly in *C. elegans*. Curr Biol 16, 1748–1756.
Gilchrist D, Mykytka B, Rexach M (2002). Accelerating the rate of disassembly of karyopherin.cargo complexes. J Biol Chem 277, 18161–18172.
Gilchrist D, Rexach M (2003). Molecular basis for the rapid dissociation of nuclear localization signals from karyopherin alpha in the nucleoplasm. J Biol Chem 278, 51937–51949.
Glavy JS, Krutchinsky AN, Cristea IM, Berke IC, Boehmer T, Blobel G, Chait BT (2007). Cell-cycle-dependent phosphorylation of the nuclear pore Nup107–160 subcomplex. Proc Natl Acad Sci USA 104, 3811–3816.
Govindaraghavan M, Lad AA, Osmani SA (2014). The NIMA kinase is required to execute stage-specific mitotic functions after initiation of mitosis. Eukaryot Cell 13, 99–109.
Guan T, Kehlenbach RH, Schirmer EC, Kehlenbach A, Fan F, Clurman BE, Arnheim N, Gerace L (2000). Nup50, a nucleoplasmically oriented nucleoporin with a role in nuclear protein export. Mol Cell Biol 20, 5619–5630.
Guttinger S, Laurell E, Kutay U (2009). Orchestrating nuclear envelope disassembly and reassembly during mitosis. Nat Rev Mol Cell Biol 10, 178–191.
Harel A, Orjalo AV, Vincent T, Lachish-Zalait A, Vasu S, Shah S, Zimmerman E, Elbaum M, Forbes DJ (2003). Removal of a single pore subcomplex results in vertebrate nuclei devoid of nuclear pores. Mol Cell 11, 853–864.
Harris SD, Morrell JL, Hamer JE (1994). Identification and characterization of *Aspergillus nidulans* mutants defective in cytokinesis. Genetics 136, 517–532.
Hartwell LH, Weinert TA (1989). Checkpoints: controls that ensure the order of cell cycle events. Science 246, 629–634.
Hase ME, Cordes VC (2003). Direct interaction with nup153 mediates binding of Tpr to the periphery of the nuclear pore complex. Mol Biol Cell 14, 1923–1940.
Hood JK, Casolari JM, Silver PA (2000). Nup2p is located on the nuclear side of the nuclear pore complex and coordinates Srp1p/importin-alpha export. J Cell Sci 113, 1471–1480.
Iouk T, Kerscher O, Scott RJ, Basrai MA, Wozniak RW (2002). The yeast nuclear pore complex functionally interacts with components of the spindle assembly checkpoint. J Cell Biol 159, 807–819.
Ishii K, Arib G, Lin C, Van Houwe G, Laemmli UK (2002). Chromatin boundaries in budding yeast: the nuclear pore connection. Cell 109, 551–562.
Jeganathan KB, Baker DJ, van Deursen JM (2006). Securin associates with APC^{Cdh1} in prometaphase but its destruction is delayed by Rae1 and Nup98 until the metaphase/anaphase transition. Cell Cycle 5, 366–370.
Jeganathan KB, Malureanu L, van Deursen JM (2005). The Rae1-Nup98 complex prevents aneuploidy by inhibiting securin degradation. Nature 438, 1036–1039.
Joseph J, Tan SH, Karpova TS, McNally JG, Dasso M (2002). SUMO-1 targets RanGAP1 to kinetochores and mitotic spindles. J Cell Biol 156, 595–602.
Kalverda B, Pickersgill H, Shloma VV, Fornerod M (2010). Nucleoporins directly stimulate expression of developmental and cell-cycle genes inside the nucleoplasm. Cell 140, 360–371.
Katsani KR, Karess RE, Dostatni N, Doye V (2008). In vivo dynamics of Drosophila nuclear envelope components. Mol Biol Cell 19, 3652–3666.
Kim MK, Claiborn KC, Levin HL (2005). The long terminal repeat-containing retrotransposon Tf1 possesses amino acids in gag that regulate nuclear localization and particle formation. J Virol 79, 9540–9555.
Kraemer D, Dresbach T, Drenckhahn D (2001). Mrnp41 (Rae 1p) associates with microtubules in HeLa cells and in neurons. Eur J Cell Biol 80, 733–740.
Laurell E, Beck K, Krupina K, Theerthagiri G, Bodenmiller B, Horvath P, Aebersold R, Antonin W, Kutay U (2011). Phosphorylation of Nup98 by multiple kinases is crucial for NPC disassembly during mitotic entry. Cell 144, 539–550.
Lee HO, Davidson JM, Duronio RJ (2009). Endoreplication: polyploidy with purpose. Genes Dev 23, 2461–2477.
Lee SH, Sterling H, Burlingame A, McCormick F (2008). Tpr directly binds to Mad1 and Mad2 and is important for the Mad1-Mad2-mediated mitotic spindle checkpoint. Genes Dev 22, 2926–2931.
Li R, Murray AW (1991). Feedback control of mitosis in budding yeast. Cell 66, 519–531.
Liang Y, Hetzer MW (2011). Functional interactions between nucleoporins and chromatin. Curr Opin Cell Biol 23, 65–70.
Lince-Faria M, Maffini S, Orr B, Ding Y, Claudia F, Sunkel CE, Tavares A, Johansen J, Johansen KM, Maiato H (2009). Spatiotemporal control of mitosis by the conserved spindle matrix protein Megator. J Cell Biol 184, 647–657.
Lindsay ME, Plafker K, Smith AE, Clurman BE, Macara IG (2002). Npap60/Nup50 is a tri-stable switch that stimulates importin-alpha:beta-mediated nuclear protein import. Cell 110, 349–360.
Liu HL, De Souza CP, Osmani AH, Osmani SA (2009). The three fungal transmembrane nuclear pore complex proteins of *Aspergillus nidulans* are dispensable in the presence of an intact An-Nup84–120 complex. Mol Biol Cell 20, 616–630.
Liu HL, Osmani AH, Ukil L, Son S, Markossian S, Shen KF, Govindaraghavan M, Varadaraj A, Hashmi SB, De Souza CP, *et al.* (2010). Single-step affinity purification for fungal proteomics. Eukaryot Cell 9, 831–833.
Loiodice I, Alves A, Rabut G, Van Overbeek M, Ellenberg J, Sibarita JB, Doye V (2004). The entire Nup107-160 complex, including three new members, is targeted as one entity to kinetochores in mitosis. Mol Biol Cell 15, 3333–3344.
Lu KP, Osmani SA, Osmani AH, Means AR (1993). Essential roles for calcium and calmodulin in G2/M progression in *Aspergillus nidulans*. J Cell Biol 121, 621–630.
Lussi YC, Shumaker DK, Shimi T, Fahrenkrog B (2010). The nucleoporin Nup153 affects spindle checkpoint activity due to an association with Mad1. Nucleus 1, 71–84.
Macaulay C, Meier E, Forbes DJ (1995). Differential mitotic phosphorylation of proteins of the nuclear pore complex. J Biol Chem 270, 254–262.
Mackay DR, Elgort SW, Ullman KS (2009). The nucleoporin Nup153 has separable roles in both early mitotic progression and the resolution of mitosis. Mol Biol Cell 20, 1652–1660.
Mackay DR, Makise M, Ullman KS (2010). Defects in nuclear pore assembly lead to activation of an Aurora B-mediated abscission checkpoint. J Cell Biol 191, 923–931.
Mackay DR, Ullman KS (2011). Coordinating postmitotic nuclear pore complex assembly with abscission timing. Nucleus 2, 283–288.
Makise M, Mackay DR, Elgort S, Shankaran SS, Adam SA, Ullman KS (2012). The Nup153-Nup50 protein interface and its role in nuclear import. J Biol Chem 287, 38515–38522.
Mans BJ, Anantharaman V, Aravind L, Koonin EV (2004). Comparative genomics, evolution and origins of the nuclear envelope and nuclear pore complex. Cell Cycle 3, 1612–1637.
Mansfeld J, Guttinger S, Hawryluk-Gara LA, Pante N, Mall M, Galy V, Haselmann U, Muhlhausser P, Wozniak RW, Mattaj IW, *et al.* (2006). The conserved transmembrane nucleoporin NDC1 is required for nuclear pore complex assembly in vertebrate cells. Mol Cell 22, 93–103.
Markina-Inarrairaegui A, Etxebeste O, Herrero-Garcia E, Araujo-Bazan L, Fernandez-Martinez J, Flores JA, Osmani SA, Espeso EA (2011). Nuclear transporters in a multinucleated organism: functional and localization analyses in *Aspergillus nidulans*. Mol Biol Cell 22, 3874–3886.
Matsuura Y, Lange A, Harreman MT, Corbett AH, Stewart M (2003). Structural basis for Nup2p function in cargo release and karyopherin recycling in nuclear import. EMBO J 22, 5358–5369.
Matsuura Y, Stewart M (2005). Nup50/Npap60 function in nuclear protein import complex disassembly and importin recycling. EMBO J 24, 3681–3689.
Mishra RK, Chakraborty P, Arnaoutov A, Fontoura BM, Dasso M (2010). The Nup107–160 complex and gamma-TuRC regulate microtubule polymerization at kinetochores. Nat Cell Biol 12, 164–169.
Musacchio A, Salmon ED (2007). The spindle-assembly checkpoint in space and time. Nat Rev Mol Cell Biol 8, 379–393.
Nayak T, Szewczyk E, Oakley CE, Osmani A, Ukil L, Murray SL, Hynes MJ, Osmani SA, Oakley BR (2006). A versatile and efficient gene-targeting system for *Aspergillus nidulans*. Genetics 172, 1557–1566.
Norden C, Mendoza M, Dobbelaere J, Kotwaliwale CV, Biggins S, Barral Y (2006). The NoCut pathway links completion of cytokinesis to spindle midzone function to prevent chromosome breakage. Cell 125, 85–98.
Oakley BR, Osmani SA (1993). Fantes P, Brooks R (1993). Cell-cycle analysis using the filamentous fungus *Aspergillus nidulans*. The Cell Cycle: A Practical Approach, Oxford, UK: Oxford University Press, 127–142.

O'Connell MJ, Meluh PB, Rose MD, Morris NR (1993). Suppression of the bimC4 mitotic spindle defect by deletion of klpA, a gene encoding a KAR3-related kinesin-like protein in *Aspergillus nidulans*. J Cell Biol 120, 153–162.

O'Connell MJ, Osmani AH, Morris NR, Osmani SA (1992). An extra copy of nimEcyclinB elevates pre-MPF levels and partially suppresses mutation of nimTcdc25 in *Aspergillus nidulans*. EMBO J 11, 2139–2149.

Ohta S, Bukowski-Wills JC, Sanchez-Pulido L, Alves F de L, Wood L, Chen ZA, Platani M, Fischer L, Hudson DF, Ponting CP, *et al*. (2010). The protein composition of mitotic chromosomes determined using multiclassifier combinatorial proteomics. Cell 142, 810–821.

Orjalo AV, Arnaoutov A, Shen Z, Boyarchuk Y, Zeitlin SG, Fontoura B, Briggs S, Dasso M, Forbes DJ (2006). The Nup107–160 nucleoporin complex is required for correct bipolar spindle assembly. Mol Biol Cell 17, 3806–3818.

Osmani AH, Davies J, Liu HL, Nile A, Osmani SA (2006a). Systematic deletion and mitotic localization of the nuclear pore complex proteins of *Aspergillus nidulans*. Mol Biol Cell 17, 4946–4961.

Osmani AH, McGuire SL, Osmani SA (1991). Parallel activation of the NIMA and $p34^{cdc2}$ cell cycle-regulated protein kinases is required to initiate mitosis in *A. nidulans*. Cell 67, 283–291.

Osmani AH, Oakley BR, Osmani SA (2006b). Identification and analysis of essential *Aspergillus nidulans* genes using the heterokaryon rescue technique. Nat Protoc 1, 2517–2526.

Osmani SA, May GS, Morris NR (1987). Regulation of the mRNA levels of nimA, a gene required for the G2-M transition in *Aspergillus nidulans*. J Cell Biol 104, 1495–1504.

Ovechkina Y, Maddox P, Oakley CE, Xiang X, Osmani SA, Salmon ED, Oakley BR (2003). Spindle formation in *Aspergillus* is coupled to tubulin movement into the nucleus. Mol Biol Cell 14, 2192–2200.

Pichler A, Gast A, Seeler JS, Dejean A, Melchior F (2002). The nucleoporin RanBP2 has SUMO1 E3 ligase activity. Cell 108, 109–120.

Pitt CW, Moreau E, Lunness PA, Doonan JH (2004). The *pot1+* homologue in *Aspergillus nidulans* is required for ordering mitotic events. J Cell Sci 117, 199–209.

Platani M, Santarella-Mellwig R, Posch M, Walczak R, Swedlow JR, Mattaj IW (2009). The Nup107–160 nucleoporin complex promotes mitotic events via control of the localization state of the chromosome passenger complex. Mol Biol Cell 20, 5260–5275.

Pontecorvo G, Roper JA, Hemmons LM, Macdonald KD, Bufton AW (1953). The genetics of *Aspergillus nidulans*. Adv Genet 5, 141–238.

Prigozhina NL, Oakley CE, Lewis AM, Nayak T, Osmani SA, Oakley BR (2004). gamma-Tubulin plays an essential role in the coordination of mitotic events. Mol Biol Cell 15, 1374–1386.

Pu RT, Osmani SA (1995). Mitotic destruction of the cell cycle regulated NIMA protein kinase of *Aspergillus nidulans* is required for mitotic exit. EMBO J 14, 995–1003.

Puig PE, Guilly MN, Bouchot A, Droin N, Cathelin D, Bouyer F, Favier L, Ghiringhelli F, Kroemer G, Solary E, *et al*. (2008). Tumor cells can escape DNA-damaging cisplatin through DNA endoreduplication and reversible polyploidy. Cell Biol Int 32, 1031–1043.

Raices M, D'Angelo MA (2012). Nuclear pore complex composition: a new regulator of tissue-specific and developmental functions. Nat Rev Mol Cell Biol 13, 687–699.

Rasala BA, Orjalo AV, Shen Z, Briggs S, Forbes DJ (2006). ELYS is a dual nucleoporin/kinetochore protein required for nuclear pore assembly and proper cell division. Proc Natl Acad Sci USA 103, 17801–17806.

Rodriguez-Bravo V, Maciejowski J, Corona J, Buch HK, Collin P, Kanemaki MT, Shah JV, Jallepalli PV (2014). Nuclear pores protect genome integrity by assembling a premitotic and mad1-dependent anaphase inhibitor. Cell 156, 1017–1031.

Schmid M, Arib G, Laemmli C, Nishikawa J, Durussel T, Laemmli UK (2006). Nup-PI: the nucleopore-promoter interaction of genes in yeast. Mol Cell 21, 379–391.

Schwartz T (2013). Functional insights from studies on the structure of the nuclear pore and coat protein complexes. Cold Spring Harb Perspect Biol 5, a013375.

Schweizer N, Ferras C, Kern DM, Logarinho E, Cheeseman IM, Maiato H (2013). Spindle assembly checkpoint robustness requires Tpr-mediated regulation of Mad1/Mad2 proteostasis. J Cell Biol 203, 883–893.

Sibthorp C, Wu H, Cowley G, Wong PW, Palaima P, Morozov IY, Weedall GD, Caddick MX (2013). Transcriptome analysis of the filamentous fungus *Aspergillus nidulans* directed to the global identification of promoters. BMC Genomics 14, 847.

Sistla S, Pang JV, Wang CX, Balasundaram D (2007). Multiple conserved domains of the nucleoporin Nup124p and its orthologs Nup1p and Nup153 are critical for nuclear import and activity of the fission yeast Tf1 retrotransposon. Mol Biol Cell 18, 3692–3708.

Smitherman M, Lee K, Swanger J, Kapur R, Clurman BE (2000). Characterization and targeted disruption of murine Nup50, a p27(Kip1)-interacting component of the nuclear pore complex. Mol Cell Biol 20, 5631–5642.

Solsbacher J, Maurer P, Vogel F, Schlenstedt G (2000). Nup2p, a yeast nucleoporin, functions in bidirectional transport of importin alpha. Mol Cell Biol 20, 8468–8479.

Steigemann P, Gerlich DW (2009). An evolutionary conserved checkpoint controls abscission timing. Cell Cycle 8, 1814–1815.

Steigemann P, Wurzenberger C, Schmitz MH, Held M, Guizetti J, Maar S, Gerlich DW (2009). Aurora B-mediated abscission checkpoint protects against tetraploidization. Cell 136, 473–484.

Stewart M (2007). Molecular mechanism of the nuclear protein import cycle. Nat Rev Mol Cell Biol 8, 195–208.

Strambio-De-Castillia C, Niepel M, Rout MP (2010). The nuclear pore complex: bridging nuclear transport and gene regulation. Nat Rev Mol Cell Biol 11, 490–501.

Suelmann R, Sievers N, Fischer R (1997). Nuclear traffic in fungal hyphae: in vivo study of nuclear migration and positioning in *Aspergillus nidulans*. Mol Microbiol 25, 757–769.

Szewczyk E, Nayak T, Oakley CE, Edgerton H, Xiong Y, Taheri-Talesh N, Osmani SA, Oakley BR (2006). Fusion PCR and gene targeting in *Aspergillus nidulans*. Nat Protoc 1, 3111–3120.

Ukil L, De Souza CC, Liu HL, Osmani SA (2009). Nucleolar separation from chromosomes during *Aspergillus nidulans* mitosis can occur without spindle forces. Mol Biol Cell 20, 2132–2145 .

Varadarajan P, Mahalingam S, Liu P, Ng SB, Gandotra S, Dorairajoo DS, Balasundaram D (2005). The functionally conserved nucleoporins Nup124p from fission yeast and the human Nup153 mediate nuclear import and activity of the Tf1 retrotransposon and HIV-1 Vpr. Mol Biol Cell 16, 1823–1838.

Waring RB, May GS, Morris NR (1989). Characterization of an inducible expression system in *Aspergillus nidulans* using alcA and tubulin-coding genes. Gene 79, 119–130.

Wente SR, Rout MP (2010). The nuclear pore complex and nuclear transport. Cold Spring Harb Perspect Biol 2, a000562.

Wong RW, Blobel G, Coutavas E (2006). Rae1 interaction with NuMA is required for bipolar spindle formation. Proc Natl Acad Sci USA 103, 19783–19787.

Xu S, Powers MA (2010). Nup98-homeodomain fusions interact with endogenous Nup98 during interphase and localize to kinetochores and chromosome arms during mitosis. Mol Biol Cell 21, 1585–1596.

Yang L, Ukil L, Osmani A, Nahm F, Davies J, De Souza CP, Dou X, Perez-Balaguer A, Osmani SA (2004). Rapid production of gene replacement constructs and generation of a green fluorescent protein-tagged centromeric marker in *Aspergillus nidulans*. Eukaryot Cell 3, 1359–1362.

Zuccolo M, Alves A, Galy V, Bolhy S, Formstecher E, Racine V, Sibarita JB, Fukagawa T, Shiekhattar R, Yen T, *et al*. (2007). The human Nup107–160 nuclear pore subcomplex contributes to proper kinetochore functions. EMBO J 26, 1853–1864.